

AD-A245 332



NAVAL POSTGRADUATE SCHOOL
Monterey, California

2



THESIS

MULTIFREQUENCY ACOUSTIC RESONATORS
WITH VARIABLE NONUNIFORMITY

by
Steven L. Alkov
June, 1991

Thesis Advisor: Bruce Denardo

Approved for public release; distribution is unlimited

92-02427



REPORT DOCUMENTATION PAGE				
1a. REPORT SECURITY CLASSIFICATION UNCLASSIFIED		1b. RESTRICTIVE MARKINGS		
2a. SECURITY CLASSIFICATION AUTHORITY		3. DISTRIBUTION/AVAILABILITY OF REPORT Approved for public release; distribution is unlimited.		
2b. DECLASSIFICATION/DOWNGRADING SCHEDULE				
4. PERFORMING ORGANIZATION REPORT NUMBER(S)		5. MONITORING ORGANIZATION REPORT NUMBER(S)		
6a. NAME OF PERFORMING ORGANIZATION Naval Postgraduate School	6b. OFFICE SYMBOL (If applicable) PH	7a. NAME OF MONITORING ORGANIZATION Naval Postgraduate School		
6c. ADDRESS (City, State, and ZIP Code) Monterey, CA 93943-5000		7b. ADDRESS (City, State, and ZIP Code) Monterey, CA 93943-5000		
8a. NAME OF FUNDING/SPONSORING ORGANIZATION	8b. OFFICE SYMBOL (If applicable)	9. PROCUREMENT INSTRUMENT IDENTIFICATION NUMBER		
8c. ADDRESS (City, State, and ZIP Code)		10. SOURCE OF FUNDING NUMBERS		
		Program Element No	Project No	Task No
				Work Unit Accession Number
11. TITLE (Include Security Classification) MULTIFREQUENCY ACOUSTIC RESONATORS WITH VARIABLE NONUNIFORMITY				
12. PERSONAL AUTHOR(S) Alkov, Steven L.				
13a. TYPE OF REPORT Master's Thesis	13b. TIME COVERED From To	14. DATE OF REPORT (year, month, day) JUNE, 1991	15. PAGE COUNT 90	
16. SUPPLEMENTARY NOTATION The views expressed in this thesis are those of the author and do not reflect the official policy or position of the Department of Defense or the U.S. Government.				
17. COSATI CODES		18. SUBJECT TERMS (continue on reverse if necessary and identify by block number)		
FIELD	GROUP	SUBGROUP		
		Acoustic resonators, Nonuniform geometry, Educational Physics, Piecewise Uniformity		
19. ABSTRACT (continue on reverse if necessary and identify by block number)				
<p>A new type of acoustic resonator utilizes alterations of the nonuniformity to achieve different resonance frequencies. Each resonator is designed to yield frequencies that correspond to musical notes. The apparatus are remarkably simple, employing piecewise uniform cross sectional areas that can easily and quickly be changed. The resonators are thus useful as educational demonstrations. The phenomenon can be understood physically and quantified perturbatively by the energy method of Rayleigh, or equivalently by the method of adiabatic invariance. Improved accuracy is obtained by matching one-dimensional solutions of the wave equation in the uniform regions. The agreement between this theory and the experimental data is less than one percent.</p>				
20. DISTRIBUTION/AVAILABILITY OF ABSTRACT <input checked="" type="checkbox"/> UNCLASSIFIED/UNLIMITED <input type="checkbox"/> SAME AS REPORT <input type="checkbox"/> DTIC USERS		21. ABSTRACT SECURITY CLASSIFICATION UNCLASSIFIED		
22a. NAME OF RESPONSIBLE INDIVIDUAL Bruce C. Denardo		22b. TELEPHONE (Include Area code) (408) 646-3485	22c. OFFICE SYMBOL PH/De	

Approved for public release; distribution is unlimited.

Multifrequency Acoustic Resonators with
Variable Nonuniformity

by

Steven L. Alkov
Lieutenant, United States Navy
B.S., Texas A&M University, 1984

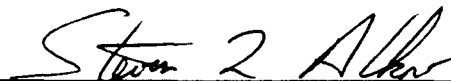
Submitted in partial fulfillment
of the requirements for the degree of

MASTER OF SCIENCE IN ENGINEERING ACOUSTICS

from the

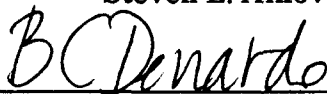
NAVAL POSTGRADUATE SCHOOL
JUNE, 1991

Author:

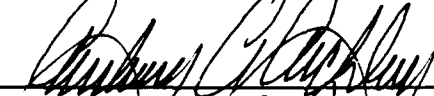


Steven L. Alkov

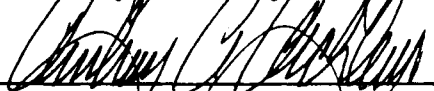
Approved by:



Bruce C. Denardo, Thesis Advisor



Anthony A. Atchley, Second Reader



Anthony A. Atchley, Chairman
Engineering Acoustics Academic Committee

ABSTRACT

A new type of acoustic resonator utilizes alterations of the nonuniformity to achieve different resonance frequencies. Each resonator is designed to yield frequencies that correspond to musical notes. The apparatus are remarkably simple, employing piecewise uniform cross sectional areas that can easily and quickly be changed. The resonators are thus useful as educational demonstrations. The phenomenon can be understood physically and quantified perturbatively by the energy method of Rayleigh, or equivalently by the method of adiabatic invariance. Improved accuracy is obtained by matching one-dimensional solutions of the wave equation in the uniform regions. The agreement between this theory and the experimental data is less than one percent.



Accession For	
NTIS SPA&I	<input checked="" type="checkbox"/>
DTIC IAB	<input type="checkbox"/>
Unannounced	<input type="checkbox"/>
Justification	
By _____	
Distribution/	
Availability Codes	
Dist	Avail and/or Special
A-1	

TABLE OF CONTENTS

I. INTRODUCTION	1
A. BACKGROUND AND MOTIVATION	1
B. DEMONSTRATIONS	4
II. THEORY	6
A. STANDARD APPROACH	6
B. SPECIAL CASES OF THE STANDARD APPROACH	13
C. RAYLEIGH'S APPROACH	16
D. ADIABATIC INVARIANCE APPROACH	23
E. HELMHOLTZ RESONATOR	26
F. WEAKLY COUPLED UNIFORM RESONATORS	29
III. DESIGN AND CONSTRUCTION	32
A. DESIGN OF THE 2-PITCH RESONATORS	32
B. DESIGN OF THE 3-PITCH RESONATORS	38
C. DESIGN OF THE 4-PITCH RESONATORS	40
D. MATERIAL	47
E. CONSTRUCTION OF RESONATORS	53
IV. EXPERIMENT	55
A. DETECTION	55
B. EXCITATION	65
C. DATA	68
D. ANALYSIS	76
V. CONCLUSIONS AND FUTURE WORK	79
A. CONCLUSIONS	79

B. FUTURE WORK 80

REFERENCES 82

INITIAL DISTRIBUTION LIST 83

ACKNOWLEDGEMENTS

I would like to express my sincerest gratitude to my thesis advisor Dr. Bruce Denardo, whose guidance, support and experimental insight made this thesis possible. Additionally, I want to acknowledge the helpful comments of Prof. Andres Larraza and Prof. Steven Baker in the theoretical and design areas of our work. Finally, special thanks to Glenn Harrell whose skill and craftsmanship produced our resonators.

I. INTRODUCTION

In this chapter, we begin with the background of and motivation for the type of resonators investigated in this thesis. Our point of view is that the resonators are primarily useful as educational demonstrations. We discuss these demonstrations in detail.

A. BACKGROUND AND MOTIVATION

The modal frequencies of any resonator depend upon the geometry of the resonator and the wave speed of the medium. (If the medium is dispersive, then the wave speed depends not only upon the medium but also the frequency.) Methods of changing the resonance frequency of a resonator fall into three categories: excitation of a different mode, alteration of the wave speed, or alteration of the geometry. A dramatic acoustics demonstration of the first is the "corrugahorn" (Crawford, 1974), and of the second is the raising or lowering of the characteristic voice frequency after helium or sulfur hexafluoride is inhaled. Common demonstrations of the third involve a change in the volume (or length) of a resonator. It is not well known that another means of changing the geometry, and thus the frequency of a mode, is to introduce or alter the nonuniformity while the volume is held constant. In the case of the one-dimensional resonator, the nonuniformity is a variation in the cross sectional area.

We have constructed simple acoustic resonators whose nonuniformity can quickly and easily be altered (Fig.I.A.1). The sound is generated by slapping one end of a single-piece resonator by hand (Szeszol, 1987) or with a rubber stopper, or by clapping together the two halves of a double-piece resonator resting on a smooth surface. The fundamental mode of these closed-open resonators is excited. By slapping the other end of a

single-piece resonator, or changing the configuration of a double-piece resonator, we effectively alter the nonuniformity and thus the frequency.

The apparatus are useful as an educational demonstration of the effects of a nonuniformity on standing waves. Each resonator is designed such that the differences in frequency correspond to musical intervals. This aides in the listeners' recognition of the change in frequency, makes the effect more dramatic, and indicates the utility of theory. In the next section we describe the demonstrations in detail. Although the phenomenon can be appreciated on an elementary level as a result of symmetry-breaking, the explanation of the effect is not elementary. In fact, our experience is that nonacousticians and even many acousticians are unable to explain the effect. In Chapter II, we give three different theoretical treatments of the problem: matching solutions of the wave equation, applying the energy method of Rayleigh, and applying the theorem of adiabatic invariance. The latter two, which are perturbative, offer physical explanations for the effect. In Chapter III, we discuss the design of the resonators, and in Chapter IV, quantitatively compare the measured frequencies to the predicted values.

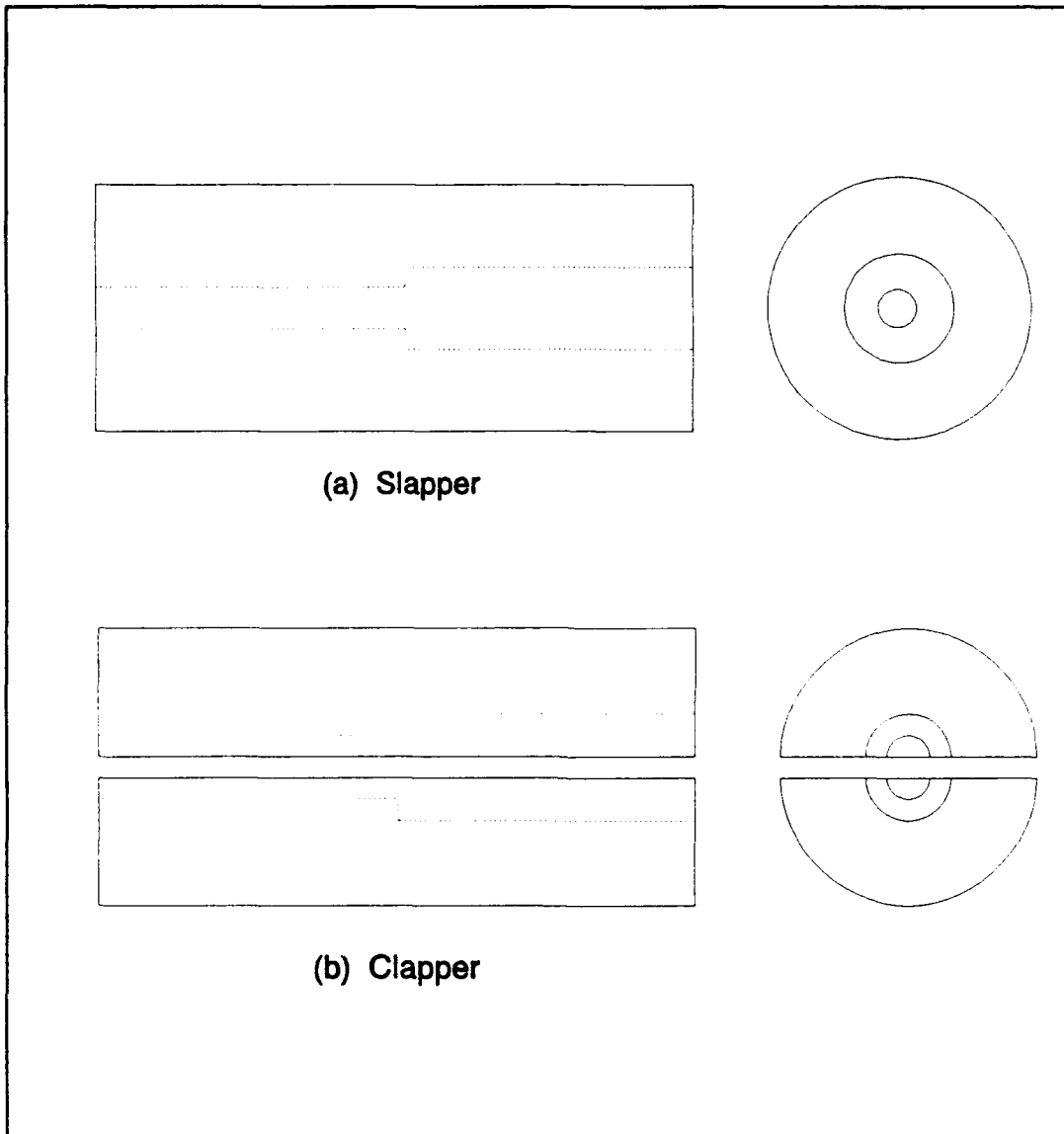


Fig.I.A.1 Variably nonuniform acoustic resonators: (a) single-piece "slapper", and (b) double-piece "clapper".

B. DEMONSTRATIONS

The following is an effective way to conduct the demonstrations. First, a single-piece resonator with uniform inner diameter is slapped by hand on one end. The sound can be easily heard in a large lecture hall. The other end is then slapped to show that the same frequency is produced, as required by symmetry. The symmetry is broken in the next resonator, which has a discontinuity in diameter (Fig.I.A.1a). The two frequencies are now different. Three such resonators are demonstrated, each with a successively greater relative difference in diameter. The first resonator is designed to have a frequency difference corresponding to a musical interval of a major third, the second resonator a perfect fifth, and the third resonator an octave.

How can an additional frequency be obtained from a resonator? If a two-pitch resonator is imagined to be cut in half along the axis (Fig.I.A.1b), there are now three distinct closed-open configurations, and thus three different frequencies will occur. Three such resonators, which correspond to halving the above three, are then demonstrated. Rather than slapping the ends, it is now convenient to clap together the two halves while one set of ends rests on a smooth surface. The first resonator yields the notes 1,2,3 of a major scale, the second resonator 1,3,5, and the third resonator 1,5,8 (in which the final frequency is an octave above the first).

Of the four possible closed-open configurations above, two are degenerate. To obtain a four-pitch resonator, we construct the two halves to be dissimilar. The symmetry is then completely broken. The final demonstration involves two four-pitch resonators that are designed to yield the eight notes of a musical scale (in which the first and final notes differ by an octave).

In all of the above demonstrations, each pitch is produced three to five times in rapid succession, so that the frequency can be implanted in the listeners' minds. This facilitates the comparison with successive frequencies.

II. THEORY

In this chapter, we develop three different approaches to determine how the frequencies of a resonator depend upon nonuniformity. Several special cases are investigated in detail.

A. STANDARD APPROACH

We consider the acoustic resonator shown in Fig.II.A.1. The problem is to determine the frequencies of the "quasilongitudinal" modes. The term refers to the fact that the flow for these modes is not purely longitudinal, due to the discontinuity in diameter. In this chapter, we assume that the length of the resonator is much greater than the characteristic diameter, so that the end correction can be neglected. The solution of the problem when $A_2 = A_1$, (or, equivalently, $\alpha = 0$ or $\alpha = 1$) is elementary. The angular frequency of the n^{th} longitudinal mode is

$$\omega_n = ck_n, \quad (\text{II.A.1})$$

where c is the speed of sound, and where the wavenumber is

$$k_n = \frac{\pi}{2L} (2n-1), \quad n=1,2,3,\dots \quad (\text{II.A.2})$$

To solve the problem when $A_2 \neq A_1$, we will assume that the flow is purely longitudinal except in a narrow region about the step. The problem then reduces to boundary condition matching of the solutions of the one-dimensional wave equation, as we now show.

We begin with the linearized one-dimensional ideal fluid equations. The linearized Euler's equation, which is a statement of Newton's Second Law, is

$$\rho_0 \frac{\partial v}{\partial t} = - \frac{\partial}{\partial x} (\delta p), \quad (\text{II.A.3})$$

where ρ_0 is the equilibrium density, v is the velocity and δp is the deviation of the pressure from the equilibrium. The linearized equation of continuity, which is a statement of mass conservation, is

$$\frac{\partial}{\partial t} (\delta \rho) + \rho_0 \frac{\partial v}{\partial x} = 0, \quad (\text{II.A.4})$$

where $\delta \rho$ is the deviation of the density from equilibrium. Equations (II.A.3) and (II.A.4) are valid if v , δp , and $\delta \rho$ are small. Under these conditions the pressure and density are related thermodynamically by

$$\delta p = c^2 \delta \rho. \quad (\text{II.A.5})$$

By eliminating $\delta \rho$ and v in (II.A.3), (II.A.4), and (II.A.5), one can readily derive the wave equation for δp :

$$\frac{\partial^2}{\partial t^2} \delta p - c^2 \frac{\partial^2}{\partial x^2} \delta p = 0. \quad (\text{II.A.6})$$

The velocity v satisfies the same equation. The wave equation (II.A.6) is valid in region 1 (to the left of the step in Fig. II.A.1) and in region 2 (to the right).

To consider standing waves, we set $\delta p = p'(x) \exp(i\omega t)$, where ω is as yet unknown. The wave equation (II.A.6) then becomes

$$\omega^2 p' + c^2 \frac{\partial^2 p'}{\partial x^2} = 0 \quad . \quad (\text{II.A.7})$$

The velocity is given by $v = v'(x) \exp(i\omega t)$, where (II.A.3) implies

$$v' = \frac{i}{\omega \rho_0} \frac{\partial p'}{\partial x} \quad . \quad (\text{II.A.8})$$

A general solution of (II.A.7) that satisfies the antinode boundary condition $\partial p' / \partial x = 0$ at $x = 0$ is

$$p'_1 = a \cos kx \quad , \quad (\text{II.A.9})$$

where ω and k are related by the dispersion law $\omega = ck$. A general solution of (II.A.4) that satisfies the node boundary condition $p' = 0$ at $x = L$ is

$$p'_2 = b \sin k(L-x) \quad . \quad (\text{II.A.10})$$

The boundary conditions at $x = \alpha L$ are that the pressure and volume velocity Av' are both continuous, where A is the cross-sectional area. By (II.A.8), the latter is equivalent to the continuity of $A\partial p' / \partial x$. Note that $\partial p' / \partial x$ is thus discontinuous for our system. By imposing the boundary conditions on (II.A.9) and (II.A.10), and dividing the resultant equations by each other in order to eliminate the amplitudes a and b , we find the wavenumber condition

$$\tan (kL\alpha) \tan [kL(1 - \alpha)] = \frac{A_2}{A_1} . \quad (\text{II.A.11})$$

The problem is to determine the values of k that satisfy this equation. The frequency ω is then given simply by the dispersion law $\omega = ck$.

For the special case $A_2 = A_1$ (no step), (II.A.11) becomes

$$\tan (kL\alpha) \tan [kL(1 - \alpha)] = 1 . \quad (\text{II.A.12})$$

This should imply the elementary solution (II.A.2). It is not even mathematically obvious that the k solution of (II.A.12) is independent of α , although we know physically that it must be. To investigate this special case, it is convenient to redefine α by letting $\alpha \rightarrow \alpha + 1/2$. Equation (II.A.12) then becomes

$$\tan [kL(1/2 + \alpha)] \tan [kL(1/2 - \alpha)] = 1 . \quad (\text{II.A.13})$$

Using the identity

$$\tan(\alpha + \beta) = \frac{\tan \alpha + \tan \beta}{1 - \tan \alpha \tan \beta} , \quad (\text{II.A.14})$$

and simplifying, we find $\tan^2(kL/2) = 1$. This implies $k = (\pi/2L)(2n-1)$, $n = 1, 2, 3, \dots$, which indeed is (II.A.2).

Equation (II.A.11) is invertible if $\alpha = 1/2$, i.e., when the step is midway between the ends of the resonator. The fractional frequency ω/ω_0 of the fundamental relative to its unperturbed ($A_2 = A_1$) value is then

$$\frac{\omega}{\omega_0} = \frac{4}{\pi} \tan^{-1} \sqrt{\frac{A_2}{A_1}} . \quad (\text{II.A.15})$$

In Fig.II.A.2, the fractional frequency shift $(\omega-\omega_0)/\omega_0$ is plotted as a function of the relative area difference $(A_2-A_1)/(A_2+A_1)$.

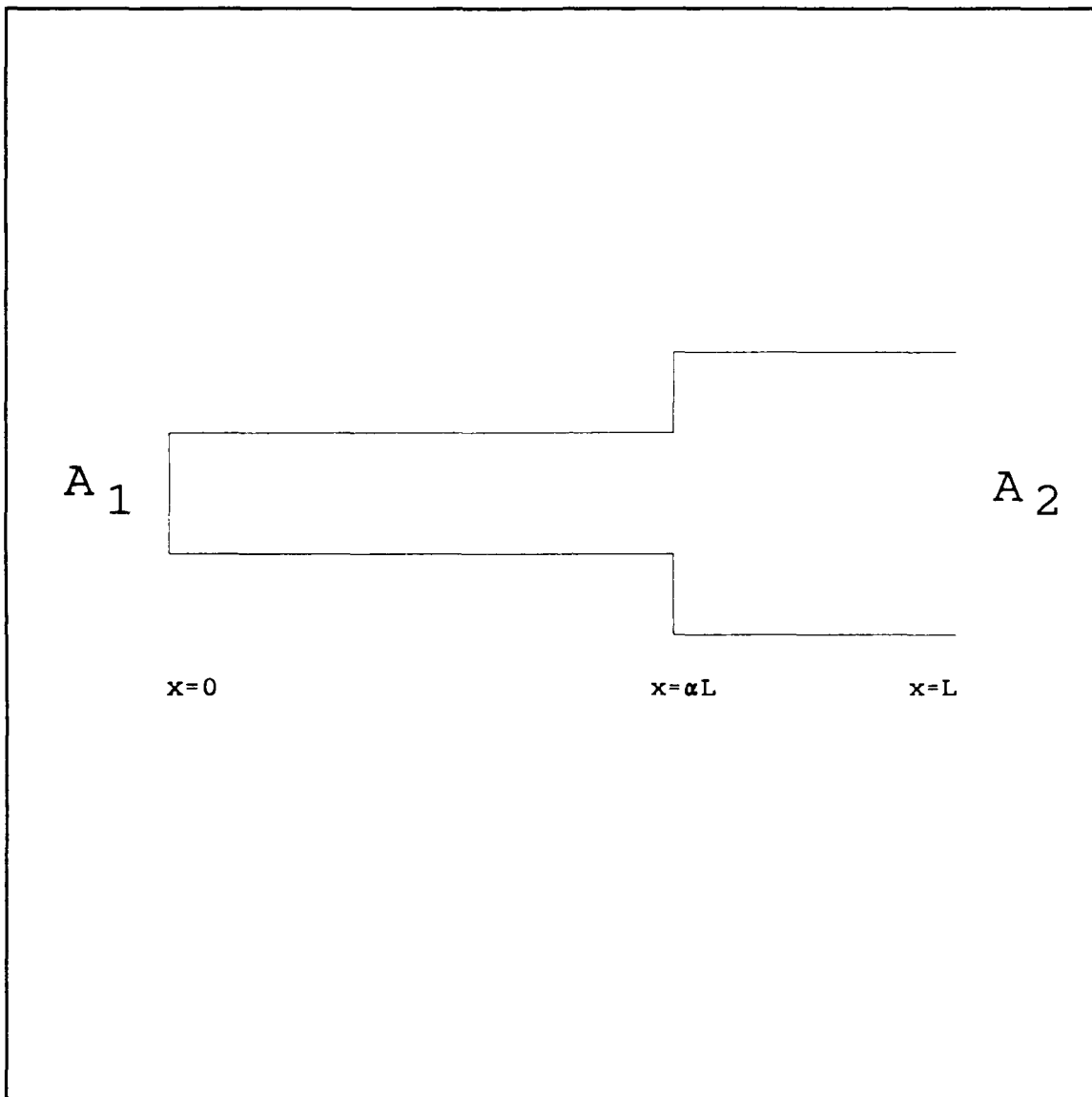


Fig.II.A.1 Geometry of the acoustic resonator. The cross sectional area equals A_1 for $0 \leq x \leq \alpha L$, and A_2 for $\alpha L \leq x \leq L$, where $0 \leq \alpha \leq 1$.

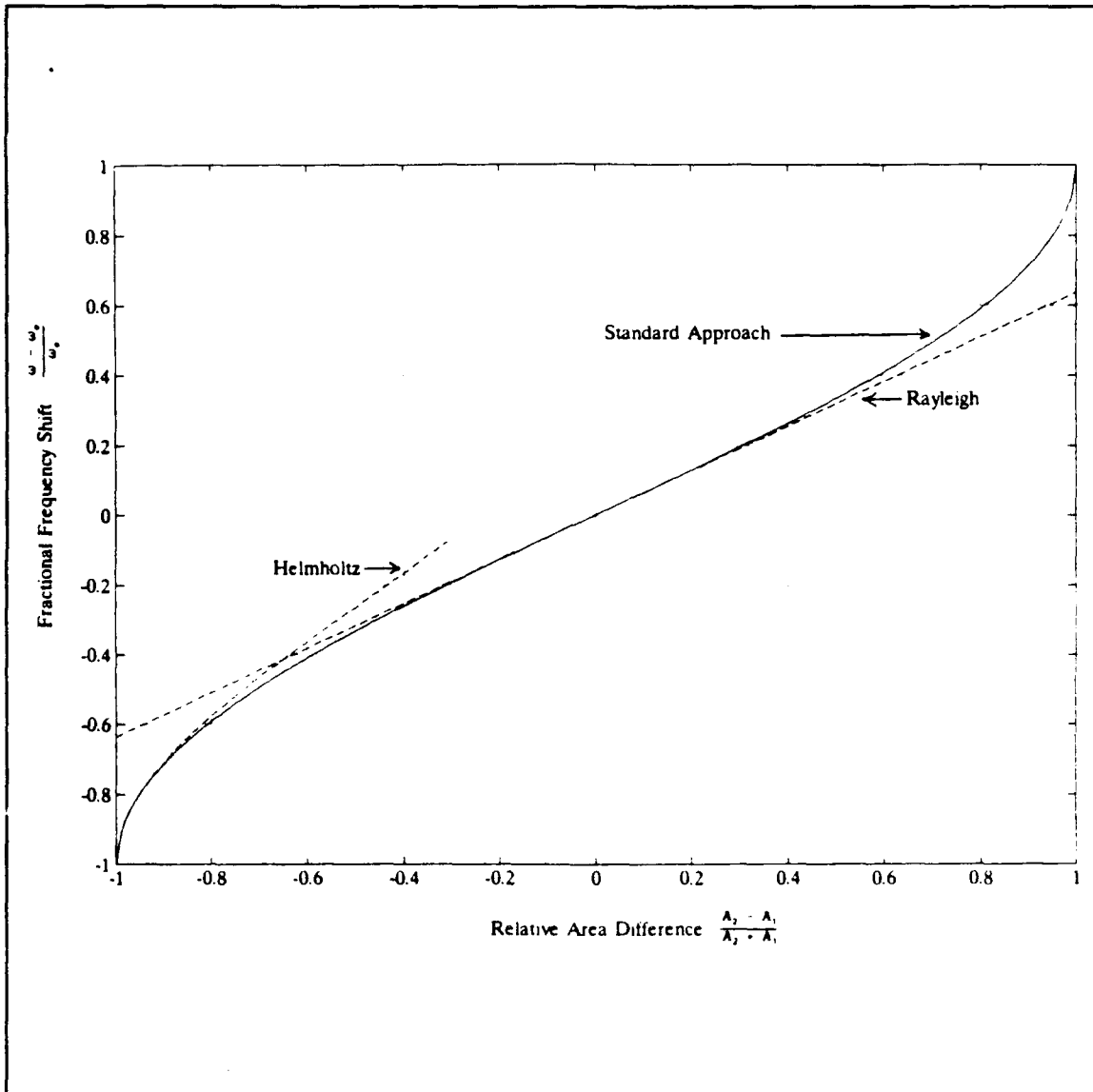


Fig.II.A.2 Fractional frequency shift of the fundamental as a function of the relative area difference for the case where the step is located halfway between the ends of the resonator.

B. SPECIAL CASES OF THE STANDARD APPROACH

In this section, we consider three special cases of the condition (II.A.11) obtained by the standard approach. The first case is a small step, the second is a large narrowing step ($A_2 \ll A_1$ in Fig.II.A.1), and the third is a large widening step ($A_2 \gg A_1$). These cases are interesting for a variety of reasons, the most important being that they can be understood qualitatively. The cases will be examined independently and thoroughly in the following paragraphs.

We now consider a small step, or the case where A_2 is approximately equal to A_1 . More precisely, this is

$$\left| \frac{A_2}{A_1} - 1 \right| \ll 1 . \quad (\text{II.B.1})$$

We refer to this as Rayleigh's case, because he derived a formula for frequency shifts due to slight nonuniformities (Section II.C).

The k solution of the condition (II.A.11) will be approximately equal to the elementary ($A_2 = A_1$) case (II.A.2). Hence, we set

$$k = k_n(1 + \epsilon) , \quad (\text{II.B.2})$$

where $|\epsilon| \ll 1$. Note that

$$\epsilon = \frac{\delta k}{k_n} , \quad (\text{II.B.3})$$

where δk is defined as $k - k_n$. We wish to determine ϵ . Once this is found, k is determined from (II.B.3), and ω is determined by

$$\frac{\delta\omega}{\omega_n} = \frac{\delta k}{k_n} , \quad (\text{II.B.4})$$

where $\delta\omega = \omega - \omega_n$. The relationship (II.B.4) follows exactly from the dispersion law $\omega = ck$. The expression (II.B.2) is substituted into the condition (II.A.11), which is then expanded to the first order in ϵ . The expansion of the tangents is given by

$$\tan [(\theta(1+\epsilon))] = \tan\theta + \epsilon\theta \sec^2\theta , \quad (\text{II.B.5})$$

which is valid for $|\epsilon| \ll 1$. After employing some elementary trigonometric identities, and simplifying, we find

$$\frac{\delta\omega}{\omega_n} = \frac{\sin[\alpha\pi(2n-1)]}{\pi(2n-1)} \left(\frac{A_2}{A_1} - 1 \right) , \quad (\text{II.B.6})$$

where we have used (II.B.3) and (II.B.4). For the fundamental ($n = 1$), this is

$$\frac{\delta\omega}{\omega_1} = \frac{\sin(\alpha\pi)}{\pi} \left(\frac{A_2}{A_1} - 1 \right) . \quad (\text{II.B.7})$$

The frequency shift $\delta\omega$ vanishes when $\alpha = 0$ or $\alpha = 1$, and is an extremum when $\alpha = 1/2$. We will derive (II.B.5) physically in later sections (II.C and II.D).

Next, we specialize the condition (II.A.11) to the case of a large narrowing step, $A_2 \ll A_1$. The system then becomes a Helmholtz resonator. For the fundamental, we can use the approximation $\tan \theta = \theta$ in the condition (II.A.11), resulting in

$$k^2 L^2 \alpha(1-\alpha) = \frac{A_2}{A_1} , \quad (\text{II.B.8})$$

which is valid for $A_2 \ll A_1$. By using the dispersion law $\omega = ck$, and solving for the frequency, we find

$$\omega^2 = c^2 \frac{A_2}{A_1} \frac{1}{L^2 \alpha (1-\alpha)} . \quad (\text{II.B.9})$$

We will show in Section II.E that this is equivalent to the well-known result obtained by directly deriving the frequency of a Helmholtz resonator.

Finally, we consider a large widening step, $A_2 \gg A_1$. In this case, the condition (II.A.11) becomes

$$[\tan kL\alpha] [\tan kL(1-\alpha)] = \infty . \quad (\text{II.B.10})$$

This implies

$$k = \frac{\pi}{2L\alpha} (2n-1) , \quad n = 1, 2, 3, \dots \quad (\text{II.B.11})$$

or

$$k = \frac{\pi}{2L(1-\alpha)} (2n-1) , \quad n = 1, 2, 3, \dots \quad (\text{II.B.12})$$

If $\alpha = 1/2$, then (II.B.11) and (II.B.12) become identical. The density of modes is thus half as much as when $\alpha \neq 1/2$. We will show in Section II.F that this degeneracy is lifted when $A_2/A_1 \neq \infty$.

C. RAYLEIGH'S APPROACH

In this section we determine the frequency shift of a mode in a closed-open resonator with a small arbitrary nonuniformity (Fig.II.C.1). The calculation is similar to that of Rayleigh (1896). The results can be easily transformed to the cases of closed-closed and open-open resonators.

The instantaneous potential and kinetic energy densities of the unperturbed mode will be denoted by $pe(x,t)$ and $ke(x,t)$, respectively. The nonuniformity $\delta A(x)$ causes the total instantaneous potential energy PE to change by the amount

$$\delta PE = \int_0^L (pe\delta A + A\delta pe) dx , \quad (\text{II.C.1})$$

where δpe is to be determined. The change in the total instantaneous kinetic energy KE is similar, except that there is an additional term due to a possible frequency shift:

$$\delta KE = \int_0^L (ke\delta A + A\delta ke) dx + 2\frac{\delta\omega}{\omega} KE . \quad (\text{II.C.2})$$

The factor of two arises because KE is proportional to the square of ω . The potential energy density is proportional to the square of the density amplitude ρ' . Furthermore, the fractional change in density amplitude equals the negative of the fractional change in volume, by continuity of mass. Hence,

$$\frac{\delta pe}{pe} = 2\frac{\delta\rho'}{\rho'} = -2\frac{\delta A}{A} . \quad (\text{II.C.3})$$

The fractional change in kinetic energy density is similarly

$$\frac{\delta ke}{ke} = 2 \frac{\delta v}{v} - 2 \frac{\delta A}{A} , \quad (\text{II.C.4})$$

where v is the velocity amplitude. Substituting (II.C.3) and (II.C.4) into (II.C.1) and (II.C.2), respectively, gives

$$\delta PE = - \int_0^L pe \delta A dx , \quad (\text{II.C.5})$$

$$\delta KE = - \int_0^L ke \delta A dx + 2 \frac{\delta \omega}{\omega} KE . \quad (\text{II.C.6})$$

For a mode executing simple harmonic motion in which all mass elements are in phase, the maximum total potential energy must equal the maximum total kinetic energy. We thus set $\delta PE_{\max} = \delta KE_{\max}$, and solve for the frequency shift. The result is

$$\frac{\delta \omega}{\omega} = \frac{1}{2E} \int_0^L (ke_{\max} - pe_{\max}) \delta A dx , \quad (\text{II.C.7})$$

where E is the total energy of the unperturbed mode. Finally, we substitute the explicit forms of the maximum energy densities:

$$pe_{\max} = \frac{2E}{AL} \cos^2 kx , \quad (\text{II.C.8})$$

$$ke_{\max} = \frac{2E}{AL} \sin^2 kx , \quad (\text{II.C.9})$$

where the wavenumber of the mode is $k = (2n-1)\pi/2L$, $n = 1, 2, 3, \dots$, for a closed-open resonator. The final result is

$$\frac{\delta\omega}{\omega} = -\frac{1}{AL} \int_0^L \cos(2kx) \delta A dx , \quad (\text{II.C.10})$$

which is equivalent to the result of Rayleigh (Rayleigh, 1945).

The effect can be understood qualitatively. Suppose that a slight constriction of small length exists at some location along the resonator. If the location is not a pressure node of the mode of interest, the potential energy of the mode will be altered. That the potential energy density exists over a smaller volume causes the potential energy to decrease. However, the density amplitude of the mode increases as a result of mass conservation, causing an increase in the potential energy. The fractional decrease in volume is identical to the fractional increase in density. Because the potential energy density is proportional to the square of the density amplitude, the magnitude of the increase in energy is twice the magnitude of the decrease. The net effect is thus an increase in potential energy. A constriction at a location that is not a pressure node therefore causes the stiffness of the mode to increase, which will raise the frequency. The opposite occurs if there is a bulge rather than a constriction. There is no effect on the stiffness if an area change is located at a pressure node. We can check the result by considering a constriction at a closed end of a resonator. The frequency indeed increases in this case, because the constriction is equivalent to a shortening of the length of the resonator.

To consider the effect upon the kinetic energy, we first note that if the location of an area change is at a velocity node, then the kinetic energy is unaltered. Otherwise, there is a competition between volume and amplitude changes analogous to the potential energy case. For a constriction, the velocity increases due to mass conservation, and the magnitude of the increase in kinetic energy is twice the magnitude of the decrease due to the volume decrease. The net effect is that a constriction at a location that is not a velocity node causes the kinetic

energy to increase. There is thus an increase in the inertia of the mode, and the frequency decreases.

In conclusion, a small constriction at a velocity node increases the stiffness and has no effect upon the inertia, so the frequency increases. At a pressure node, a small constriction increases the inertia and has no effect upon the stiffness, so the frequency decreases. The effects compete if the area alteration is at neither a velocity nor pressure node. In the case where the cross sectional area continuously changes along the length of the resonator such that the deviation from the mean value is always small, the frequency shift is the integral over differential shifts due to area changes of differential length.

In addition to being physical, Rayleigh's energy method is in general very useful as a means of determining the frequency shifts due to small nonuniformities. For example, it has been applied to the modes of a bar whose ends have additional mass due to transduction coils (Garrett, 1990).

The Rayleigh formula (II.C.10) exhibits a symmetry that is important in the design of our resonators. If the closed and open ends are switched, note that $\delta\omega/\omega$ simply changes sign. There thus exists a reflection antisymmetry. If a resonator is composed of two halves, there are then four possible closed-open orientations and thus four frequencies (which may not be distinct). As a result of the reflection antisymmetry, however, the relationships of the frequencies is not arbitrary.

To quantify this, we define the functional

$$\gamma_1 = -\frac{1}{AL} \int_0^L \cos(2kx) \delta A_1 dx , \quad (\text{II.C.11})$$

and similarly γ_2 , where $\delta A_1(x)$ and $\delta A_2(x)$ are the variations in cross sectional area of the halves that compose the resonator. The total variation is $\delta A = \delta A_1 + \delta A_2$. The fractional frequency shifts $\delta\omega/\omega$ corresponding to the four orientations are then $\pm(\gamma_1+\gamma_2)$ and $\pm(\gamma_1-\gamma_2)$. Without loss of generality, we assume that $\gamma_1, \gamma_2 \geq 0$ and $\gamma_2 \geq \gamma_1$. For a fixed function $\delta A_2(x)$, and thus a fixed value of γ_2 , we consider different

functions $\delta A_1(x)$ such that $0 \leq \gamma_1 \leq \gamma_2$. This explores all possible relationships among the four frequencies. The results are shown in Fig.II.C.2. The orientations of the two halves are labeled by arrows. We have arbitrarily labeled the lowest frequency orientation by two down arrows. The degenerate cases in Fig.II.C.2 can occur as follows. If one of the halves is uniform, then $\delta A_1 = 0$ and thus $\gamma_1 = 0$. There are then only two frequencies. If both halves are identical, then $\delta A_1 = \delta A_2$ and thus $\gamma_1 = \gamma_2$. There are then only three frequencies. These special cases assume that $\gamma_2 \neq 0$.

Finally, we specialize the Rayleigh formula (II.C.10) to the case of the fundamental mode of our piecewise uniform resonator (Fig.II.A.1). After integrating and simplifying, we find

$$\frac{\delta\omega}{\omega} = \frac{A_2 - A_1}{A} \frac{\sin \pi\alpha}{\pi} . \quad (\text{II.C.12})$$

This is valid if the relative difference between A_1 and A_2 is small. The reference area A can be chosen as any value that roughly equals A_1 (or A_2). (Deviations in (II.C.10) or (II.C.12) due to the choice of A are beyond the accuracy of the result.) Comparison of (II.C.12) with the special case (II.B.7) of the standard result shows that the two are equivalent to the order of the approximation. For $\alpha = 1/2$ and $A = (A_1 + A_2)/2$, a plot the Rayleigh result is shown in Fig.II.A.2. Note that it closely approximates the standard result over a broad range of differences in the areas.

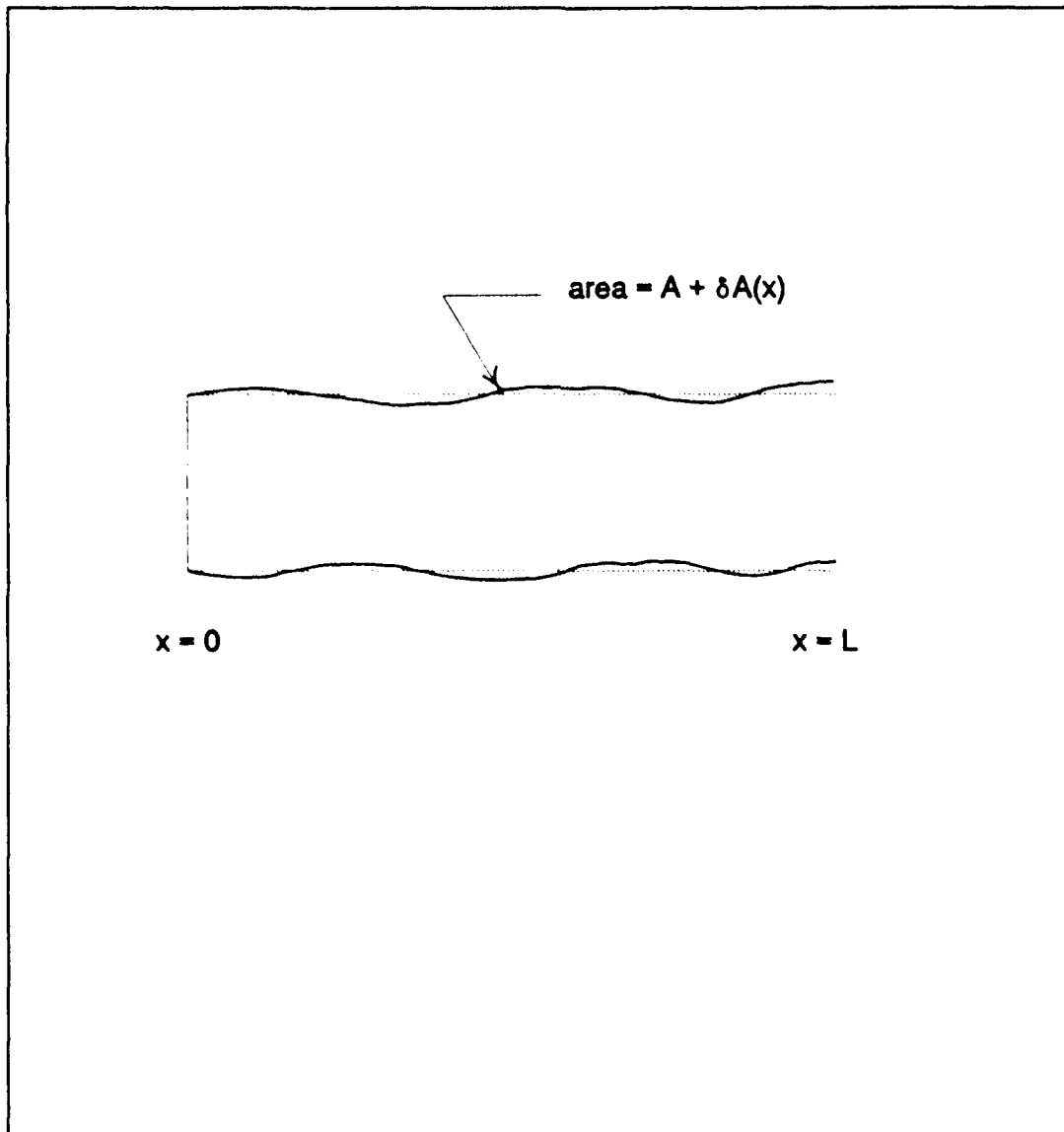


Fig.II.C.1 Closed-open resonator with a small arbitrary nonuniformity.

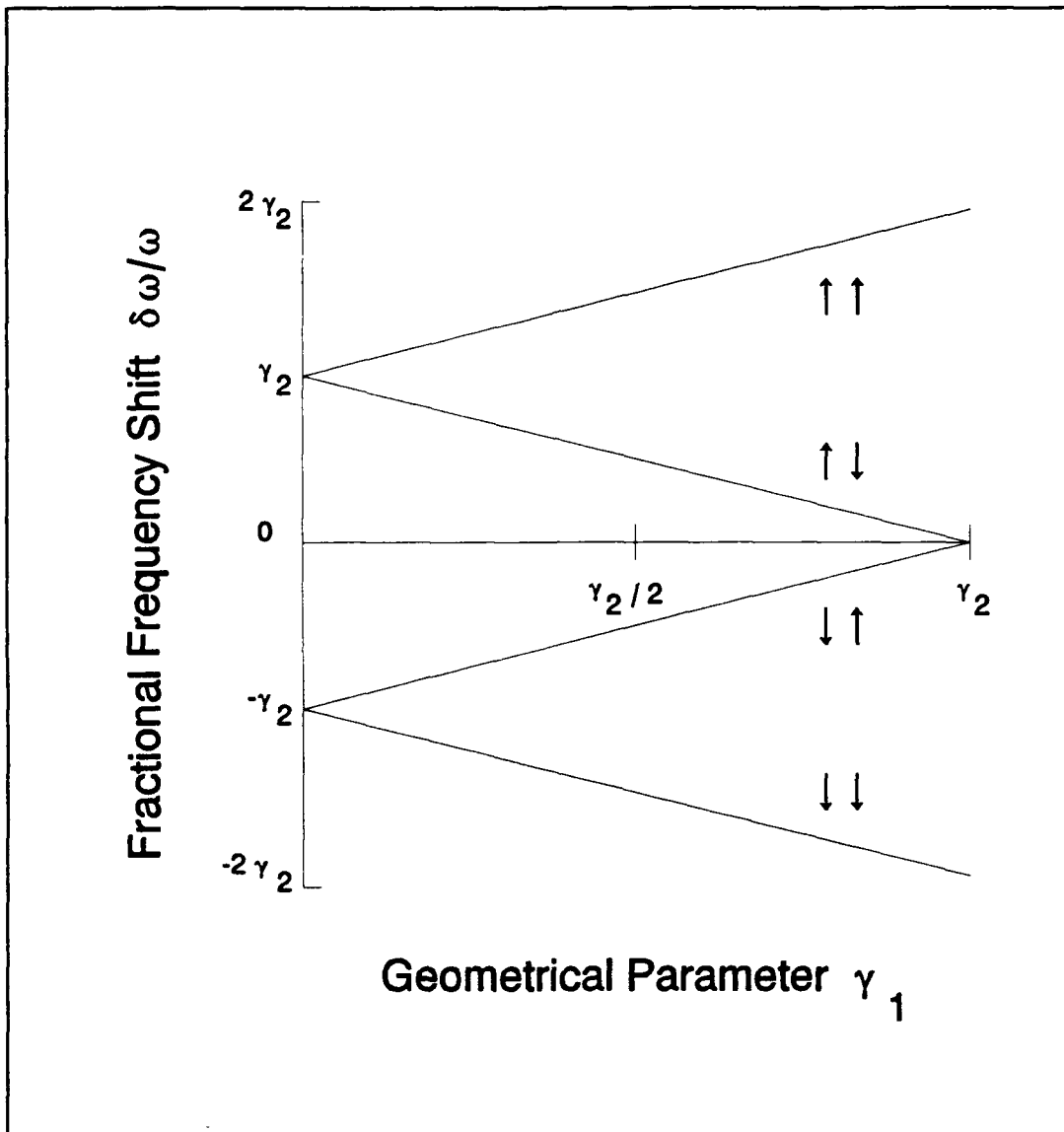


Fig.II.C.2. Fractional frequency splittings of an open-closed resonator composed of two halves.

D. ADIABATIC INVARIANCE APPROACH

In the expression (II.C.7), we observe that the frequency shift due to a perturbation in cross sectional area at a location depends only upon the relative difference of the potential and kinetic energy densities at that location. One might wonder if this is a general result which applies in any geometry (including higher dimensions). By employing adiabatic invariance, we now show that this is indeed true.

We consider any mode of an arbitrary cavity. To neglect end effects due to possible openings, we assume that either the cavity is completely closed or that periodic boundary conditions occur. (The latter is appropriate for the case of our one-dimensional closed-open resonator.) Suppose that the mode has energy E and frequency ω , and that dissipation is neglected. We now imagine that an external agent slowly deforms the surface of the cavity by a small amount, such that the displacement at every point is perpendicular to the surface. By the theorem of adiabatic invariance, energy remains in a single mode. Because the motion is simple harmonic, the adiabatic invariant is the quotient of the energy and the frequency (Crawford, 1990). Hence, in the perturbative case,

$$\frac{\delta\omega}{\omega} = \frac{\delta E}{E} , \quad (\text{II.D.1})$$

where $\omega + \delta\omega$ is the new frequency and $E + \delta E$ is the new energy.

The change in energy δE equals the work δW done by the external agent. If \bar{p} is the time-averaged pressure, dS is an element of surface area, and $\delta\xi$ is the displacement, the work is

$$\delta W = \oint \bar{p} ds \delta \xi , \quad (\text{II.D.2})$$

where the integration is over the surface of the cavity. To second order in the amplitude of the sound field, the time-averaged pressure is (Landau and Lifshitz, 1959)

$$\bar{p} = p_0 + p_{rad} + \text{const} , \quad (\text{II.D.3})$$

where the radiation pressure on the surface of the cavity is

$$p_{rad} = \frac{1}{2} (pe_{max} - ke_{max}) . \quad (\text{II.D.4})$$

In these expressions, p_0 is the equilibrium pressure, and pe_{max} and ke_{max} are the maximum potential and kinetic energy densities at a point. The second term in the radiation pressure (II.D.4) is the familiar Bernoulli pressure that also arises in incompressible flow. The first term is an additional pressure that arises due to the compressibility. In the time-averaged pressure (II.D.3), the constant is necessary in order to keep the total mass fixed, because there is also a second order time-averaged density which is in general nonzero.

The part of the work (II.D.2) due to the pressure $p_0 + \text{const}$ corresponds to a change in the overall density, and therefore to a change in temperature. We ignore this part of the work because we desire the frequency shift due to geometrical and not temperature alteration. By combining (II.D.1), (II.D.2), (II.D.3), and (II.D.4), we find that this frequency shift is

$$\frac{\delta\omega}{\omega} = \frac{1}{2E} \oint (pe_{\max} - ke_{\max}) dS \delta\xi \quad . \quad (\text{II.D.5})$$

To apply this to the case of a one-dimensional resonator that is initially uniform, we set $dS\delta\xi = dx\delta A$, where dx is an element of length of the resonator and $\delta A(x)$ is the variation in the cross sectional area. The result (II.D.5) is then identical to the intermediate result (II.C.7) in Rayleigh's case.

Adiabatic invariance offers an elegant explanation of the frequency shift due to nonuniformity of a resonator. In fact, we can view the frequency shift as an indirect demonstration of adiabatic invariance. On a practical level, the method predicts the frequency shift when an arbitrarily complicated geometry is altered a small amount at a point. All that is required is the relative difference of the potential and kinetic energy densities at that point.

E. HELMHOLTZ RESONATOR

In the limit $A_2 \ll A_1$, our piecewise uniform resonator (Fig.II.A.1) becomes a Helmholtz resonator. In this section, we directly derive the frequency of this resonator, and show that the result is equivalent to the limiting case of our general result.

The geometry of a Helmholtz resonator is shown in Fig.II.E.1. The frequency can be determined by applying Newton's Second Law to the mass of the fluid in the neck. The amount of this mass is

$$m = \rho h A , \quad (\text{II.E.1})$$

where ρ is the density. If the volume hA of the neck is much less than the volume V of the cavity, the fluid in the neck then oscillates rigidly and the fluid in the cavity contracts and expands uniformly. The excess force exerted by the fluid in the cavity on the fluid in the tube is

$$F = A p' , \quad (\text{II.E.2})$$

where p' is the excess pressure in the cavity. Using $p' = c^2 \rho'$, where ρ' is the excess density in the cavity, and

$$\frac{\rho'}{\rho} = \frac{V'}{V} = -\frac{A x}{V} , \quad (\text{II.E.3})$$

we can express (II.E.2) as

$$F = -\frac{A^2 x}{V} . \quad (\text{II.E.4})$$

Substituting this and (II.E.1) into $F = m d^2 x / d^2 t$ gives

$$\frac{d^2x}{dt^2} + \frac{c^2A}{hV} x = 0 , \quad (\text{II.E.5})$$

from which we find the frequency:

$$\omega^2 = \frac{c^2A}{hV} . \quad (\text{II.E.6})$$

This is the standard expression for the frequency of a Helmholtz resonator. To apply (II.E.6) to the geometry of our piecewise uniform resonator (Fig.II.A.1), we set $A = A_2$, $h = (1-\alpha)L$, and $V = A_1\alpha L$. These yield

$$\omega^2 = c^2 \frac{A_2}{A_1} \frac{1}{L^2\alpha(1-\alpha)} . \quad (\text{II.E.7})$$

This is identical to (II.B.9), which is our general result evaluated in the limit $A_2 \ll A_1$.

We can express (II.E.7) in dimensionless variables by employing the unperturbed frequency, which is $\omega_0 = \pi c/2L$. Then,

$$\frac{\omega}{\omega_0} = \frac{2}{\pi} \sqrt{\frac{A_2}{A_1}} \frac{1}{\sqrt{\alpha(1-\alpha)}} . \quad (\text{II.E.8})$$

This is plotted in Fig.II.A.2 together with the standard result and the Rayleigh approximation. The standard result connects the Helmholtz and Rayleigh cases.

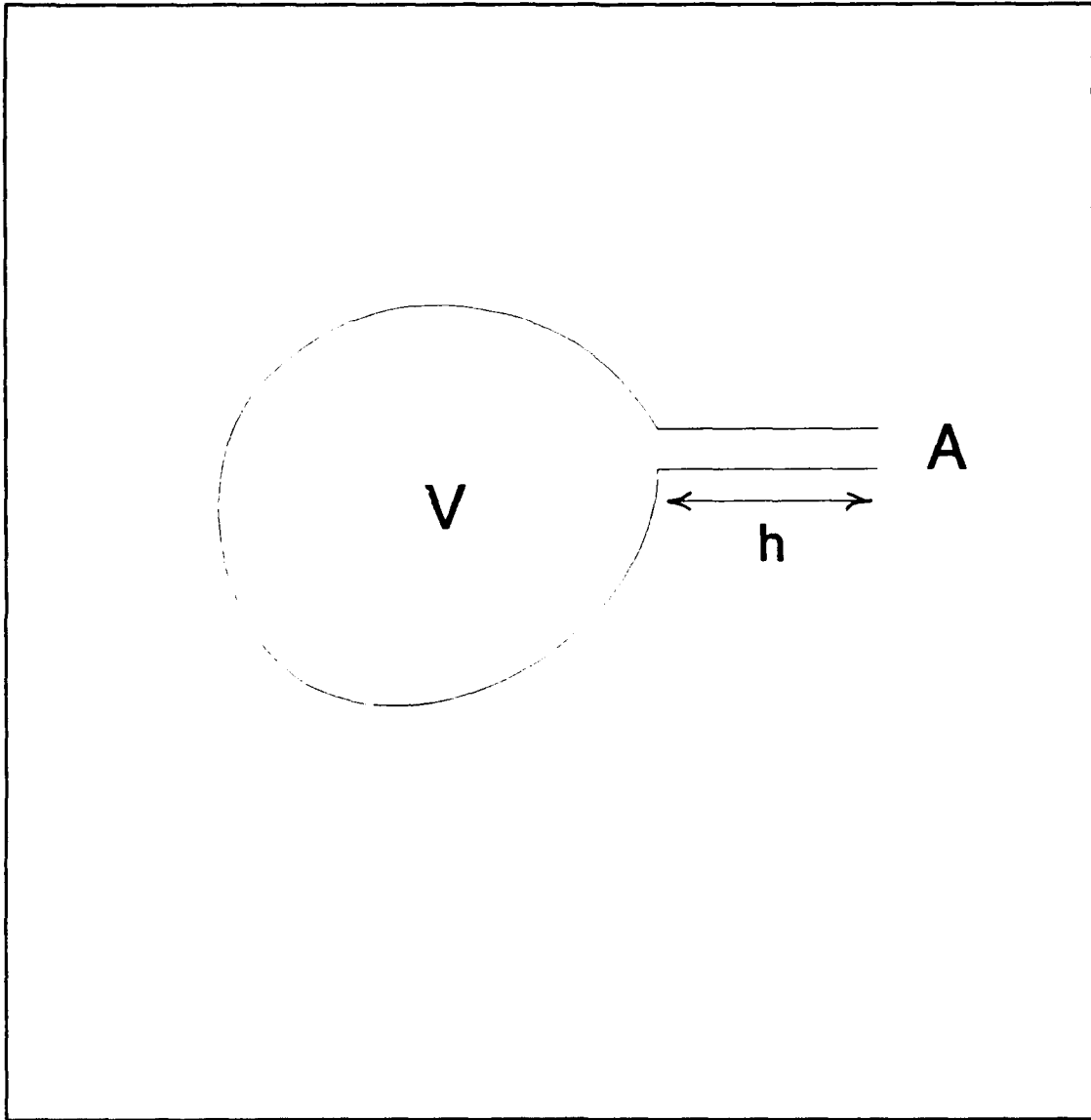


Fig.II.E.1 Geometry of a Helmholtz resonator.

F. WEAKLY COUPLED UNIFORM RESONATORS

In this section we consider the case of a large widening step, $A_2 \gg A_1$, in Fig.II.A.1. We found in (II.B.10) and (II.B.11) that when $A_2/A_1 = \infty$ in the condition (II.A.11), the frequency spectrum is the union of the two simple spectra of uniform resonators of length αL and $(1-\alpha)L$. In this limiting situation, therefore, we effectively have two uncoupled uniform resonators. This is reasonable physically: the resonator with the small cross sectional area A_1 , which has one closed end, has its other end effectively completely open. Similarly, the resonator with the large cross sectional area A_2 , which has one open end, has its other end effectively completely closed. Fig.II.F.1 shows the frequency spectrum as a function of the step location α , where $0 \leq \alpha \leq 1$. The dashed curves correspond to the limiting case $A_2/A_1 = \infty$, in which there are two uncoupled uniform resonators.

When $1 \ll A_2/A_1 < \infty$, these uniform resonators become weakly coupled. In this case, we determine the spectrum by numerically solving (II.A.11). The solid curves in Fig.II.F.1 correspond to $A_2/A_1 = 20$. The phenomenon of mode level repulsion occurs in the regions where the uncoupled (dashed) curves intersect: the weak coupling lifts the degeneracy here. The situation is essentially the same as in the elementary case of two weakly coupled identical oscillators. The piecewise uniform resonator in fact offers one of the simplest examples of mode level repulsion in a continuum.

Finally, we comment on the nature of the spectrum in Fig.II.F.1 when A_2 is not much greater than A_1 . When $A_2 = A_1$, the solid curves become horizontal lines at the values $\omega/\omega_0 = 1, 3, 5, \dots$. (This is the elementary case of a uniform resonator.) When $A_2/A_1 \ll 1$, we again have two weakly coupled resonators, but now the boundary conditions for each resonator are not mixed. (One resonator is approximately open-open; the other closed-closed.) The uncoupled spectrum curves are thus hyperbolas as before, but

now they have the values $\omega/\omega_0 = 2, 4, 6, \dots$ when $\alpha = 0$ or $\alpha = 1$. The fundamental is the Helmholtz mode, and the higher modes will exhibit the level repulsion effect mentioned above. Note that the curves must still have the values $\omega/\omega_0 = 1, 3, 5, \dots$ when $\alpha = 0$ or $\alpha = 1$, however. Near these values of α the coupling ceases to be weak; the boundary conditions are no longer approximately unmixed.

The numerical solution that yields the solid curves in Fig.II.F.1 is not standard and should thus be explained. The problem can be posed as the determination of values of ω/ω_0 such that $f(\omega/\omega_0, \alpha) = 0$, where

$$f\left(\frac{\omega}{\omega_0}, \alpha\right) = \tan\left(\frac{\pi}{2} \frac{\omega}{\omega_0} \alpha\right) \tan\left[\frac{\pi}{2} \frac{\omega}{\omega_0} (1 - \alpha)\right] - \frac{A_2}{A_1} .$$

There are an infinite number of such zeros (or roots), where the first lies between $\omega/\omega_0 = 0$ and $\omega/\omega_0 = 2$, the second between 2 and 4, the third between 4 and 6, etc. The bisection method is thus preferable to Newton's method. A problem with the bisection method, however, is that f has poles. To the bisection method, these appear as roots. The problem cannot be removed by redefining f such that the tangents appear in the denominator, because now the zeros of the tangents give rise to poles. Our trick is to multiply f by functions that have simple zeros where f has its (simple) poles. Specifically, to determine the five curves in Fig.II.F.1, we use bisection to solve $p_1 p_2 f = 0$, where the prefactors are

$$p_1 = \left(\frac{\omega}{\omega_0} \alpha - 1\right) \left(\frac{\omega}{\omega_0} \alpha - 3\right) \dots \left(\frac{\omega}{\omega_0} \alpha - 9\right) ,$$

$$p_2 = \left[\frac{\omega}{\omega_0} (1 - \alpha) - 1\right] \left[\frac{\omega}{\omega_0} (1 - \alpha) - 3\right] \dots \left[\frac{\omega}{\omega_0} (1 - \alpha) - 9\right] .$$

Note that this technique does not alter the values of the roots.

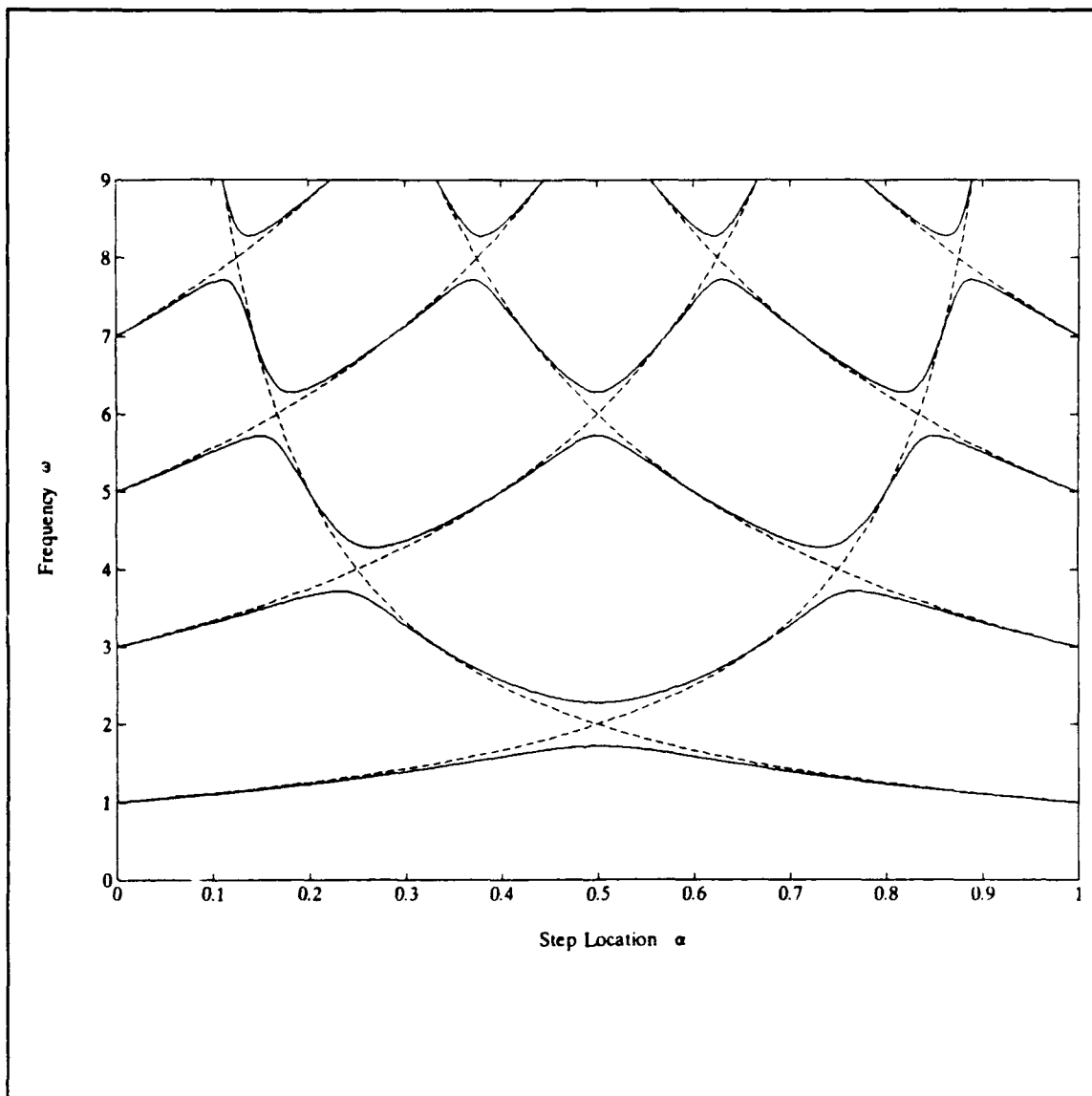


Fig.II.F.1 Frequency spectrum of a piecewise uniform resonator when $A_2/A_1 = 20$ (solid curves), and $A_2/A_1 = \infty$ (dashed curves).

III. DESIGN AND CONSTRUCTION

In this chapter, we discuss the design and construction of the resonators such that the ratios of the frequencies will approximately equal musical values. Despite the simple appearance of the resonators, we will show that neither the design nor construction are easily accomplished.

A. DESIGN OF THE 2-PITCH RESONATORS

By a "two-pitch" resonator we mean a single-piece resonator that is slapped by hand at one end and then the other. Because this switches the boundary conditions on the acoustic field, we have seen that a nonuniform resonator will in general have two different frequencies. In this section we discuss the design of these resonators (called "slappers") such the ratio of the frequencies corresponds to a musical interval.

An octave is an interval from one frequency to twice that frequency. In the equal-tempered musical scale, an octave is split into twelve intervals that are equally spaced with respect to the logarithm of the frequency. This is necessary if a sequence of frequencies (or notes) is to be perceived as essentially the same regardless of the key (or first frequency of the scale). Let f_n , $n = 0, 1, 2, \dots, 12$, be the frequencies of a chromatic scale. Equal temperment implies

$$\log f_n = \log f_0 + \frac{n}{12} (\log f_{12} - \log f_0) . \quad (\text{III.A.1})$$

Substituting $f_{12} = 2f_0$, simplifying, and exponentiating, yields

$$f_n = 2^{\frac{n}{12}} f_0 . \quad (\text{III.A.2})$$

The relative frequencies f_n/f_0 are tabulated in Table III.A.1. We have labeled the frequencies not by n , but by the notes corresponding to the major scale, which is the sequence 1,2,3,4,5,6,7,8. We will design slappers whose frequency ratios are 3, 5, and 8. The two generated notes can thus be denoted as 1-3, 1-5, and 1-8, which is how we will label the resonators.

The simplest nonuniformity to impose is a step in an otherwise uniform resonator (Fig.II.A.1) We investigated this case in Section II.A. If the end correction is neglected, the relationship between frequency and the geometry is given by Equation (II.A.11). For a fixed discontinuity in the cross sectional area, the greatest frequency shift occurs when the step is halfway between the ends of the resonator. We accordingly choose this case. Furthermore, we assume circular cross sectional areas. Equation (II.A.11) then reduces to

$$\tan\left(\frac{\omega L}{2c}\right) = \frac{d_2}{d_1}, \quad (\text{III.A.3})$$

where we have used the dispersion law $\omega = ck$, and where d_1 and d_2 are the diameters corresponding to the areas A_1 and A_2 , respectively. Slapping the other end causes the boundary conditions to be switched, which inverts the right side of (III.A.3) and thus leads to a different frequency. We refer to the two frequencies as ω_1 and ω_2 , where $\omega_1 > \omega_2$, and to the diameters as d_1 and d_2 , where $d_1 > d_2$. We wish to determine values of d_1 and d_2 such that ω_1/ω_2 is a desired value in Table III.A.1.

First, we must consider the effect of the end correction. The length of the resonators is six inches, the outer diameter is three inches, and the characteristic inner diameter is one inch. Because the wavelength is much larger than the wall thickness of the resonator, the end correction amounts to the addition of the length $\delta L = 0.305d$ to the geometrical length L , where d is the open-end diameter (Pierce, 1989). We now show that the end correction causes two errors, each of which reduces the ratio

of the two frequencies. In (III.A.3) the frequency is inversely proportional to the length L . However, due to the different diameters, the values of the effective length are different for the two cases. Because the open end in the case of the ω_1 frequency has a greater diameter than that in the ω_2 case, the ratio ω_1/ω_2 will be reduced due to the end effect. This is the dominant effect. The secondary effect is due to the fact that the end correction causes the step to no longer lie halfway between the ends of the resonator. (It is nearer to the closed end.) This also causes a reduction of ω_1/ω_2 because the ratio is greatest when the step is halfway between the ends. Due to the fact that this is an extremum, however, the value of ω_1/ω_2 is relatively insensitive to the location of the step as long as it is near the center.

We will include the dominant effect of the end correction, but will neglect the secondary effect. Hence (III.A.3) can still be used if the length L is replaced by $L + 0.305d_2$. The ratio of the frequencies is then given by

$$\frac{\omega_1}{\omega_2} = \frac{1 + \frac{0.305d_1}{L} \tan^{-1}\left(\frac{d_1}{d_2}\right)}{1 + \frac{0.305d_2}{L} \tan^{-1}\left(\frac{d_2}{d_1}\right)} \quad \text{(III.A.4)}$$

This cannot be inverted. However, because the end effect is small, we can solve for values of d_1 and d_2 by first determining these values when the end correction is omitted, and then using these as starting values in a numerical search. Without the end correction, (III.A.4) is

$$\frac{\omega_+}{\omega_-} = \frac{\tan^{-1}(\frac{d_+}{d_-})}{\tan^{-1}(\frac{d_-}{d_+})} \quad (III.A.5)$$

We can invert this by using the identity $\tan^{-1}(1/x) = \pi/2 - \tan^{-1}(x)$. Solving (III.A.5) for d_+/d_- then gives

$$\frac{d_+}{d_-} = \tan\left(\frac{\Delta}{1+\Delta} \frac{\pi}{2}\right) \quad (III.A.6)$$

where $\Delta = \omega_+/\omega_-$. It should be noted that the analytical determination of d_+/d_- without the end correction is only possible if the step is located halfway between the ends. Otherwise, a numerical solution is required.

Using (III.A.6), we determine d_+/d_- for the values of Δ corresponding to the musical intervals 1-3, 1-5, and 1-8 in Table III.A.1. Next, we uniquely determine d_+ and d_- by arbitrarily choosing their mean value to be unity, which will be taken to as one inch in the construction of the resonators. Finally, these values are employed as a starting point in a simple numerical search to determine the values of d_+ and $d_- = 2-d_+$ to the nearest 0.001 that satisfy the more accurate equation (III.A.4). This is quickly accomplished with only a hand calculator.

The resultant values of d_+ and d_- are tabulated in Table III.A.2. To ensure that these diameters yield values of Δ that are accurate to less than 1%, the tolerance of the diameters should be ± 0.002 inches. From Table III.A.1, a minor second (or half step) corresponds to about a 6% increase in Δ , so we consider deviations less than 1% to be acceptable.

One may wonder if the Rayleigh approximate result (II.C.12) would yield sufficiently accurate diameters. The best way to investigate this is to assume the values of the diameters in Table III.A.2, substitute them into the Rayleigh result, determine the corresponding values of $\Delta = \omega_+/\omega_-$, and compare these to the musical values in Table III.A.1. When this is

done, the deviation is found to be 0.1% for the 1-3 resonator, 0.7% for the 1-5, and 3.4% for the 1-8. The Rayleigh approximation is thus sufficient except in the final case. It should be noted that the Rayleigh approximation would be much less accurate if we did not employ the average area $A = (A_1 + A_2)/2$ as the reference area in the derivation in Section II.C.

Table III.A.1 Relative frequencies of the notes of the chromatic scale.

Musical Note	Relative Frequency	Musical Note	Relative Frequency
1	1	5	1.4983
1#	1.0595	6b	1.5874
2	1.1225	6	1.6818
3b	1.1892	7b	1.7818
3	1.2599	7	1.8877
4	1.3348	8	2
4#	1.4142		

Table III.A.2 Diameters of 2-pitch and 3-pitch resonators whose lengths are $L = 6.000$ inches.

Resonator	Diameter (inches)	Diameter (inches)
1-3 and 1-2-3	1.094	0.906
1-5 and 1-3-5	1.164	0.836
1-8 and 1-5-8	1.278	0.722

B. DESIGN OF THE 3-PITCH RESONATORS

If we imagine cutting a 2-pitch resonator in half along the axis, an additional configuration (and therefore an additional frequency) is now possible. Furthermore, slapping is no longer necessary. If one end of the resonator is set on a smooth horizontal surface, and the thumbs are used as hinges where the edge of the halves meet, we can clap the halves together to produce sound. These resonators are referred to as "clappers." How can we design these resonators to approximately yield musical frequency intervals?

The answer is simple. If a slapper is imagined to be cut in half, the new frequency will approximately equal the average of the original frequencies. Now, the musical notes 2, 3, and 5 lie approximately halfway between 1 and 3, 1 and 5, and 1 and 8, respectively.

To quantitatively investigate the deviation of the middle frequency from the desired musical value, we calculate the frequency ratio

$$\frac{\omega_o}{\omega_i} = \frac{1 + \frac{0.305d_i}{L}}{1 + \frac{0.305d_{rms}}{L}} \frac{\frac{\pi}{4}}{\tan^{-1}\left(\frac{d_i}{d_i}\right)}, \quad (\text{III.B.1})$$

where d_{rms} is the root-mean-square diameter of the end when the diameters are mixed:

$$d_{rms} = \left(\frac{d_i^2 + d_i^2}{2} \right)^{1/2}. \quad (\text{III.B.2})$$

This is the appropriate value to use in the end correction, because it is the diameter corresponding to the circle whose area equals that of the slapper. For $L = 6.000$ inches, and for the slapper diameters in Table III.A.2, the deviations of the middle frequencies from the desired musical values are tabulated in Table III.B.1. Remarkably, the deviations are all

less than 1%, which meets our design criterion. Hence, we will employ this design. Of course, we should not physically cut the slapper in half, because some material will be loss. The effective diameters would then be less than the original values, and the frequencies would shift. The actual construction of the 3-pitch clappers is discussed in Section III.E.

Table III.B.1 Comparison of the theoretical middle frequencies of the 3-Pitch resonators to the desired musical values.

Resonator	Relative Middle Frequency ω_o/ω	Desired Musical Value	Deviation
1-2-3	1.1302	1.1225	+ 0.69%
1-3-5	1.2502	1.2599	- 0.77%
1-5-8	1.5043	1.4983	+ 0.40%

C. DESIGN OF THE 4-PITCH RESONATORS

By constructing dissimilar halves of a clapped resonator, we can produce four different frequencies. It is then possible to design two resonators such that one gives the first four notes of a musical scale, and the other gives the latter four notes. In this case, we know from our experience with the previous resonators that the step sizes will be small. Using the Rayleigh theory as a guide, we then find that we do not have the freedom to approximate a major scale. In fact, the symmetry of the frequency splittings (Fig.II.C.2) restricts the possibilities among standard scales to the harmonic minor (Fig.III.C.1). In this section, we comment on a design of a pair of four-pitch resonators that approximately yield this scale.

One way to make the halves of a resonator different is construct the steps to lie at different locations. This would significantly increase the difficulty of the theoretical calculations, however. A simpler way is to keep both steps at the middle of the resonator, but to alter the cross sectional areas (Fig.III.C.2). Equation (III.A.4) thus still applies. As encountered in Section III.B, however, d_1 and d_2 are now the root-mean-square (rms) values of the semicircular diameters a_1 and b_1 . For the configuration shown in Fig.III.C.2, $d_1^2 = (a_1^2 + b_1^2)/2$ and $d_2^2 = (a_2^2 + b_2^2)/2$. For the first resonator we will choose diameters such that the outer two frequencies differ by a perfect fourth (P4) musical interval, and the inner two by a minor second (m2). For the second resonator, we choose P4 and m3 (minor third). These are diagrammed in Fig.III.C.3. The intervals between the first and second frequencies, and the third and fourth, will then only approximately equal the desired musical values. We will later calculate the deviations, and show that they are acceptable. Also, we will later calculate the lengths of the resonators such that the second resonator yields the latter four notes of the scale.

To obtain the P4 interval, we set

$$\mu_i^2 = \frac{a_i^2 + b_i^2}{2} , \quad (\text{III.C.1})$$

where μ_i are diameters that yield a P4 interval. To obtain the m2 (or m3) interval, we set

$$\nu_i^2 = \frac{a_i^2 + b_i^2}{2} , \quad (\text{III.C.2})$$

where ν_i are diameters that yield a m2 (or m3) interval. Equations (III.C.1) and (III.C.2) are four equations in the four unknowns a_i and b_i . However, they are not consistent unless an area constraint is satisfied:

$$\mu_i^2 + \mu_j^2 = \nu_i^2 + \nu_j^2 , \quad (\text{III.D.3})$$

which states that the total area (of both ends) must be independent of the configuration. This is not satisfied if the mean values of μ_i and μ_j , or ν_i and ν_j , are chosen to be unity, as we did before. We can satisfy (III.C.3) by now choosing the rms values to be unity:

$$\mu_{rms} = 1 = \nu_{rms} . \quad (\text{III.C.4})$$

Equations (III.C.2) and (III.C.3) then become redundant. In particular, we are free to conveniently choose

$$a_{rms} = 1 = b_{rms} . \quad (\text{III.C.5})$$

The solution is then given by

$$\begin{aligned} a_1^2 &= \mu_1^2 + \nu_1^2 - 1 , \\ b_1^2 &= \mu_1^2 - \nu_1^2 + 1 . \end{aligned} \tag{III.C.6}$$

By the procedure established in Section III.A, we find $\mu_1^2 = 1.2315$ for a P4 interval and $\nu_1^2 = 1.1405$ for a m3, both for a resonator of length $L = 6$ inches. We show below that the length of the second resonator must be $L = 9.142$ inches. We then find $\mu_2^2 = 1.2290$ for a P4 interval, and $\nu_2^2 = 1.0465$ for a m2. The resultant values of the diameters a_2 and b_2 for both resonators are tabulated in Table III.C.1.

We have now designed two 4-pitch resonators whose outer and inner frequency intervals are correct. We must determine how accurate are the intervals between the first and second frequencies, as well as the third and fourth. This can be accomplished as in Section III.B. The results are that the frequencies deviate by about 1% from the musical values. As stated in Section III.B, we consider this to be acceptable because the notes of a m2 interval (the smallest) deviate by 6%.

Finally, we must determine lengths of the two resonators such that the second will yield the notes 5, 6, 7, and 8 relative to the first, which has the notes 1, 2, 3, and 4 (Fig. III.C.3) Hence, we demand that

$$f_6 = \beta f_1 , \tag{III.C.7}$$

where $\beta = 1.4983$ (which corresponds to a perfect fifth). The frequency splittings of each resonator are symmetrical about the central values f_1 and f_{11} . These are the frequencies of the unperturbed (uniform cross sectional area) resonators. Because the outer frequencies of each resonator have the same ratio, it must be that $f_6/f_{11} = f_1/f_1$ or

$$\frac{f_6}{f_1} = \frac{f_{II}}{f_I} . \quad (\text{III.C.8})$$

Now, the ratio of the unperturbed frequencies is

$$\frac{f_{II}}{f_I} = \frac{L_I + \delta L}{L_{II} + \delta L} , \quad (\text{III.C.9})$$

where L_I and L_{II} are the lengths of the resonators, and δL is the end correction (0.305 multiplied by the open-end diameter). Combining (III.C.7), (III.C.8), and (III.C.9), we find that we must choose the lengths of the resonators such that

$$\beta = \frac{L_I + \delta L}{L_{II} + \delta L} . \quad (\text{III.C.10})$$

We set $L_{II} = 6.000$ inches and approximate the diameter as 1.000 inch. The end correction is thus $\delta L = 0.305$. Solving for L_I gives

$$L_I = \beta L_{II} + (\beta - 1) \delta L , \quad (\text{III.C.11})$$

which yields $L_I = 9.142$ inches. The effect of the end correction here is about 2%, which is not negligible according to our 1% criterion.

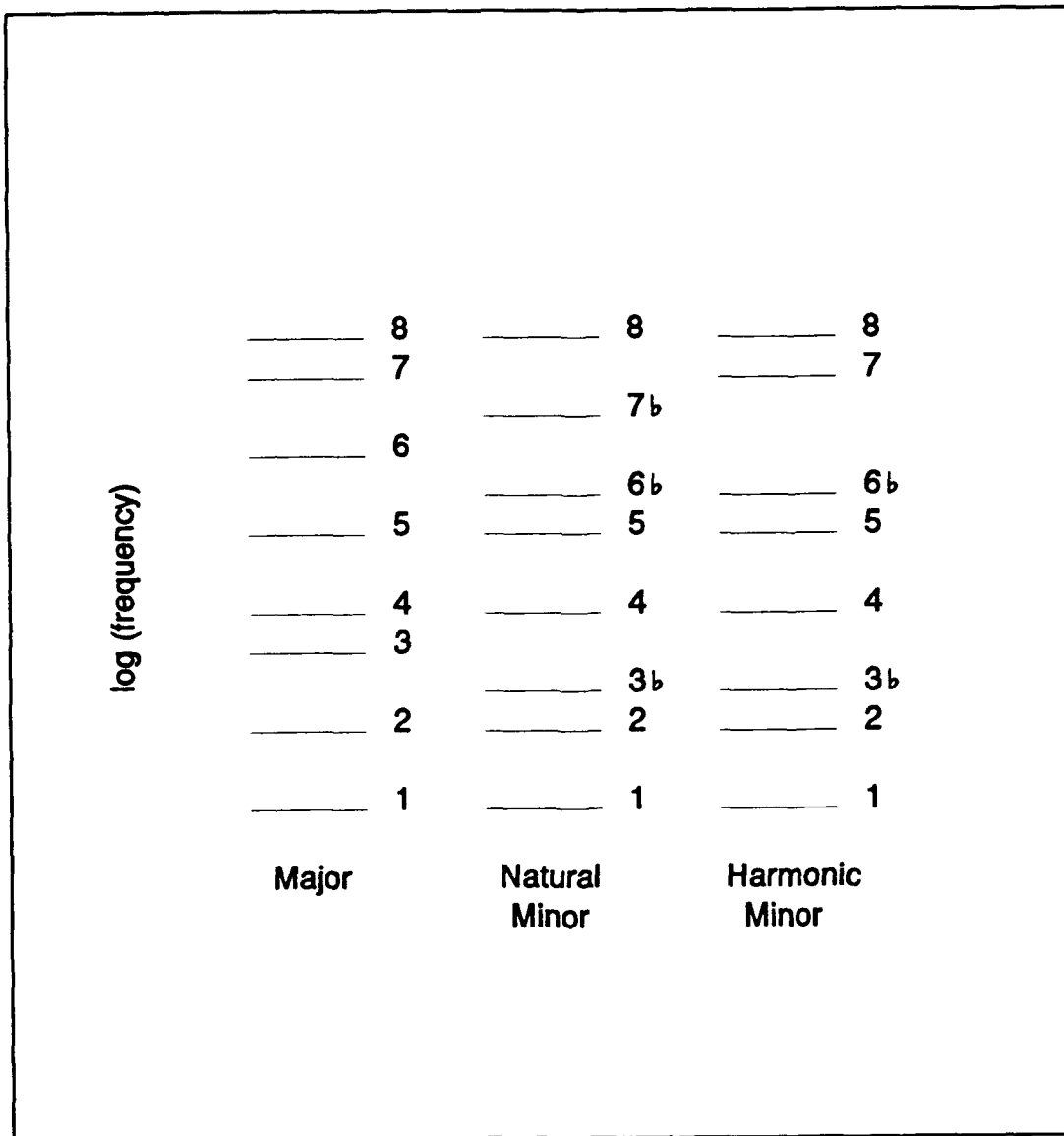


Fig.III.C.1 Standard musical scales. The 4-pitch resonator is conducive to the harmonic minor scale.

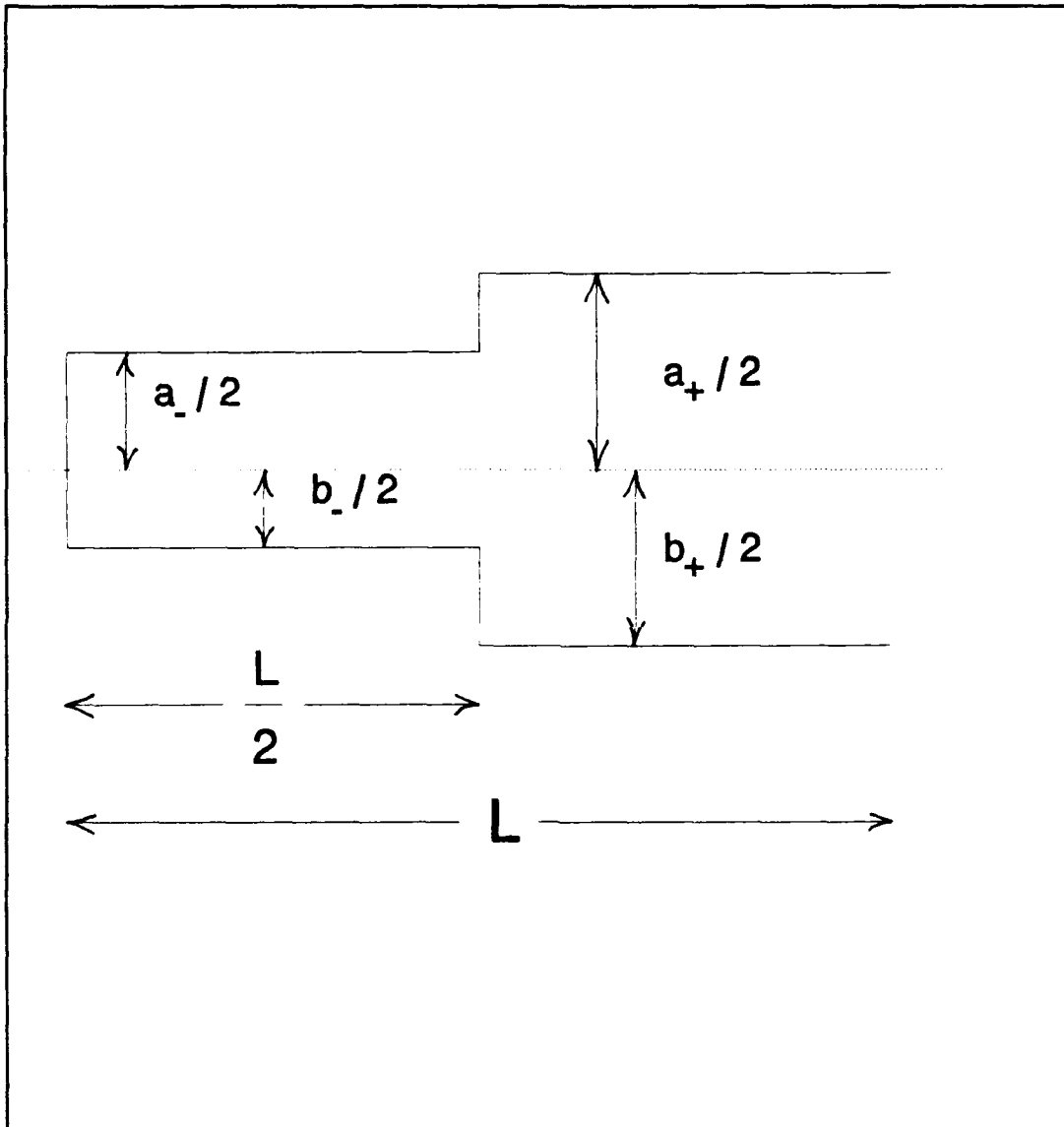


Fig.III.C.2 Geometry of a 4-pitch resonator. The quantities a_- and b_- are diameters.

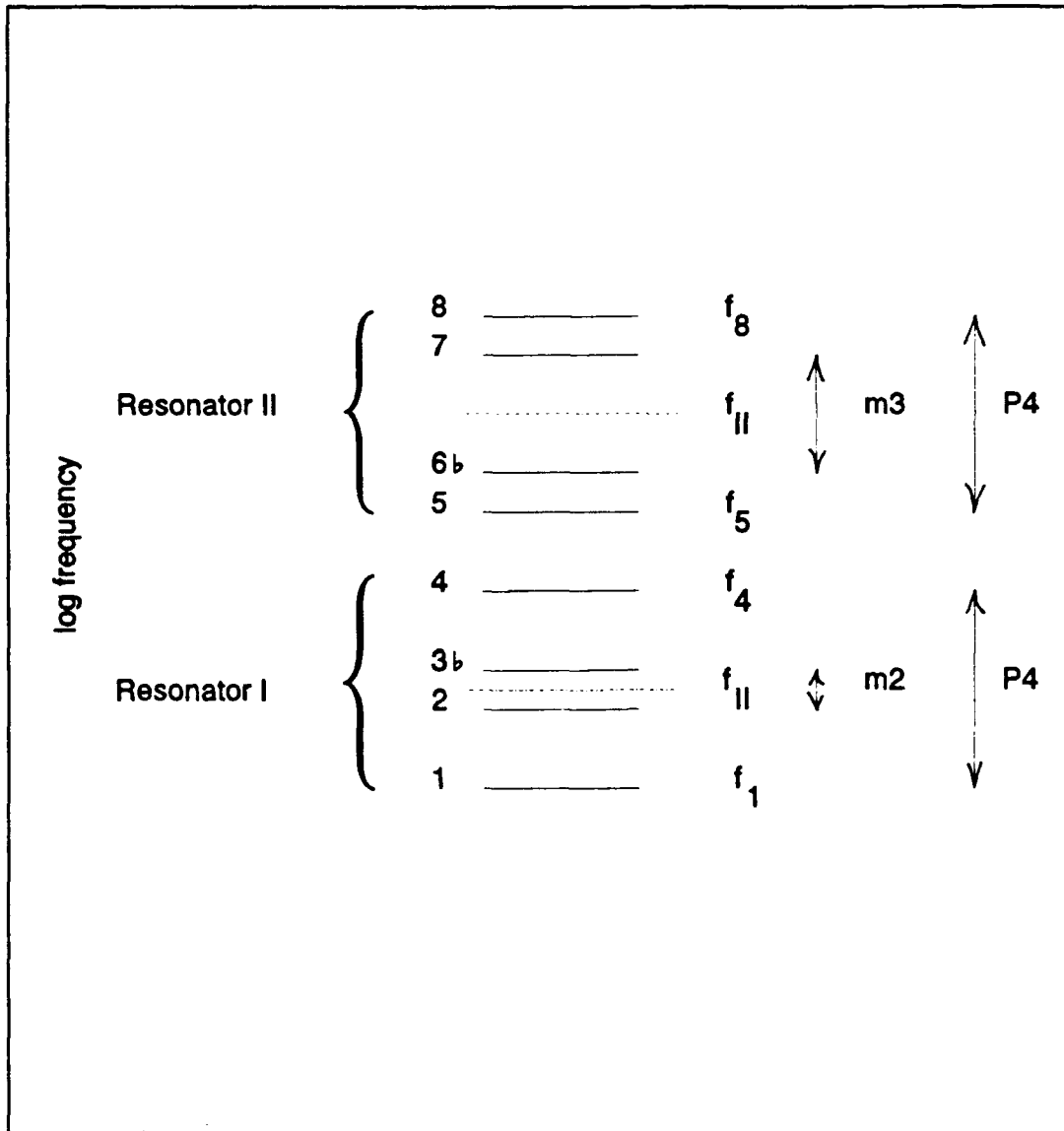


Fig.III.C.3 Frequency diagram for the 2-pitch resonators that yield a harmonic minor scale.

Table III.C.1 Dimensions of a set of 4-pitch resonators that yield a harmonic minor scale.

Resonator	Length (inches)	Diameters (inches)	Diameters (inches)
1-2-3b-4	9.142	1.129, 0.851	1.087, 0.904
5-6b-7-8	6.000	1.171, 0.792	1.045, 0.953

D. MATERIAL

The desire to obtain experimental results that would best demonstrate the theory, as previously discussed in Chapter II, established a criterion for the basic requirements of this thesis. To achieve our criterion, acoustic resonators had to be constructed out of a material which would produce resonators of sufficient quality to meet our needs. There were several factors in the selection of the construction material for the resonators. The most important factor was the desire to produce the cleanest signal and clearest tone possible without the use of an excessive excitation force. The use of an excessive excitation force could lead to over ringing and reverberation of harmonics of the resonant frequency. The result of an excessive excitation force can be seen in Fig.III.D.1. The beating of the resonant frequency is clearly evident. Additionally, the cost, availability, and inherent manufacturing difficulties of the different materials (as will be discussed in Section III.E), were also contributing factors in our decision.

Several acoustic resonators of both the two-pitch (slapper) and three-pitch (clapper) variety were constructed out of different materials in order to determine the best material for this research. The two different methods of exciting the resonators (Section I.B) provided a means to determine which of the materials would be acceptable for use in constructing the resonators. Based on tests conducted with slappers constructed from acrylic and wood (fir), the tone quality was found not to

be dependent on the material of the slapper, as expected. Additionally, the quality of the free decay time series plot were also similar. However, the fir proved to be a more difficult material to machine than the acrylic. This was apparent when a comparison of the fir slapper to the acrylic slapper showed that the critical interior walls of the fir resonator did not bore as smoothly. Since the tolerances of the interior diameters were ± 0.002 inches (Section III.A), sanding of the interior wall smoother was not a viable option. Furthermore, from a demonstration viewpoint, the clear acrylic allows one to view the step in the resonator. Based on these considerations, the material of choice for the two-pitch slappers was acrylic.

The excitation signal of the clappers was created from the hitting (or clapping) of the two symmetric halves flush onto each other (Section I.B). Here, unlike the slappers, the resulting excitation signal is dependent on the material of the clapper. The first clapper produced was machined from a stock of aluminum. The higher density of the aluminum allowed the excitation of usable signals with only a minimum use of force. However, the tone quality of the resonator was poor due to the highly metallic ring of the signal. As with the slappers, the second choice for a construction material was acrylic. The acrylic proved to be a very acceptable choice of material for construction. This was due to the fact that the excitation of a clean signal with purer tone quality, using a minimum amount of force, was more easily reproduced.

The need to insure that a more acceptable material was not overlooked resulted in a clapper constructed from maple. While the maple, being denser than fir, made for easier machining, the maple clapper did not produce a signal as clean nor with as long of a useable record length as the acrylic clappers. Comparison of Fig.III.D.2 (a 1-2-3 resonator made from maple) and Fig.III.D.3 (a 1-2-3 resonator constructed from acrylic) clearly demonstrates the better signal quality of acrylic versus maple.

The tone quality of the maple clapper also was inferior to the acrylic. These factors again pointed toward the acrylic as the material of choice. It should be noted that several more exotic woods such as rosewood and mahogany were considered but due to the exorbitant cost of these exotic woods they were disregarded. These would probably yield a sound similar to the maple. Therefore, acrylic was selected to be the construction material for all of the resonators.

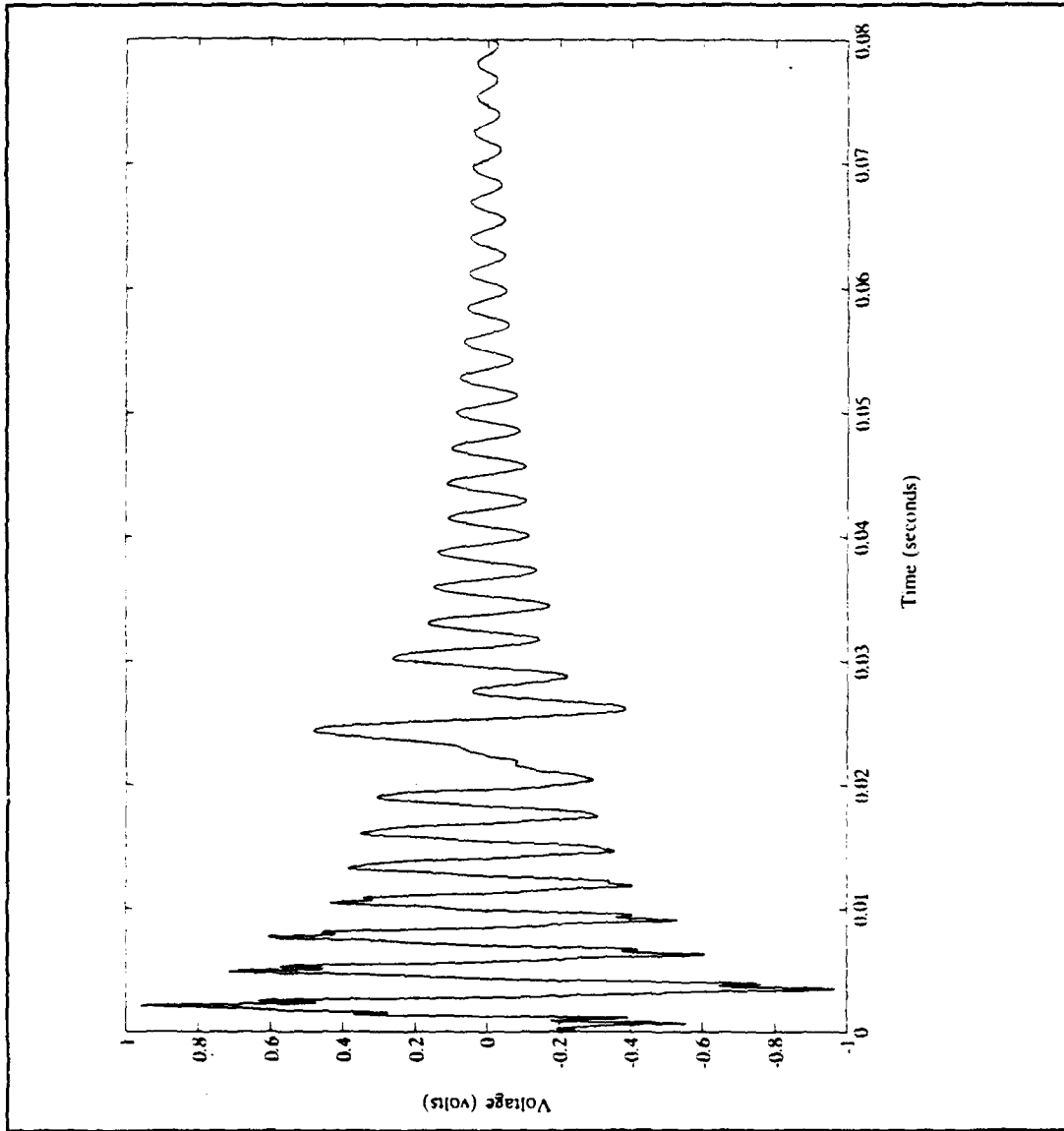


Fig.III.D.1 Example of beating of signal due to use of an excessive excitation force for the 1-8 slapper resonator.

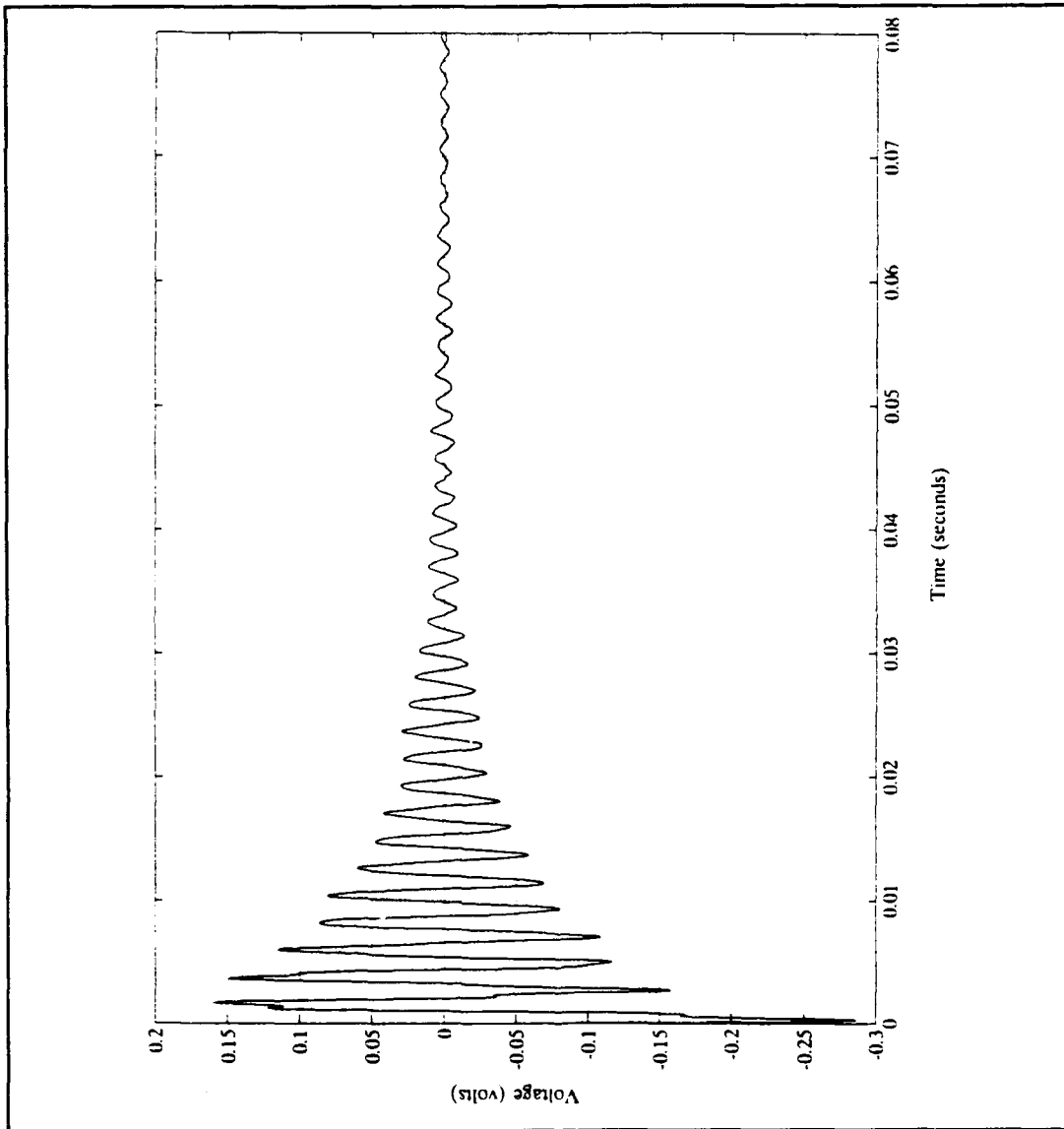


Fig.III.D.2 Time series plot of a 1-2-3 clapper resonator constructed from maple. Note the deterioration of the signal after 40 ms.

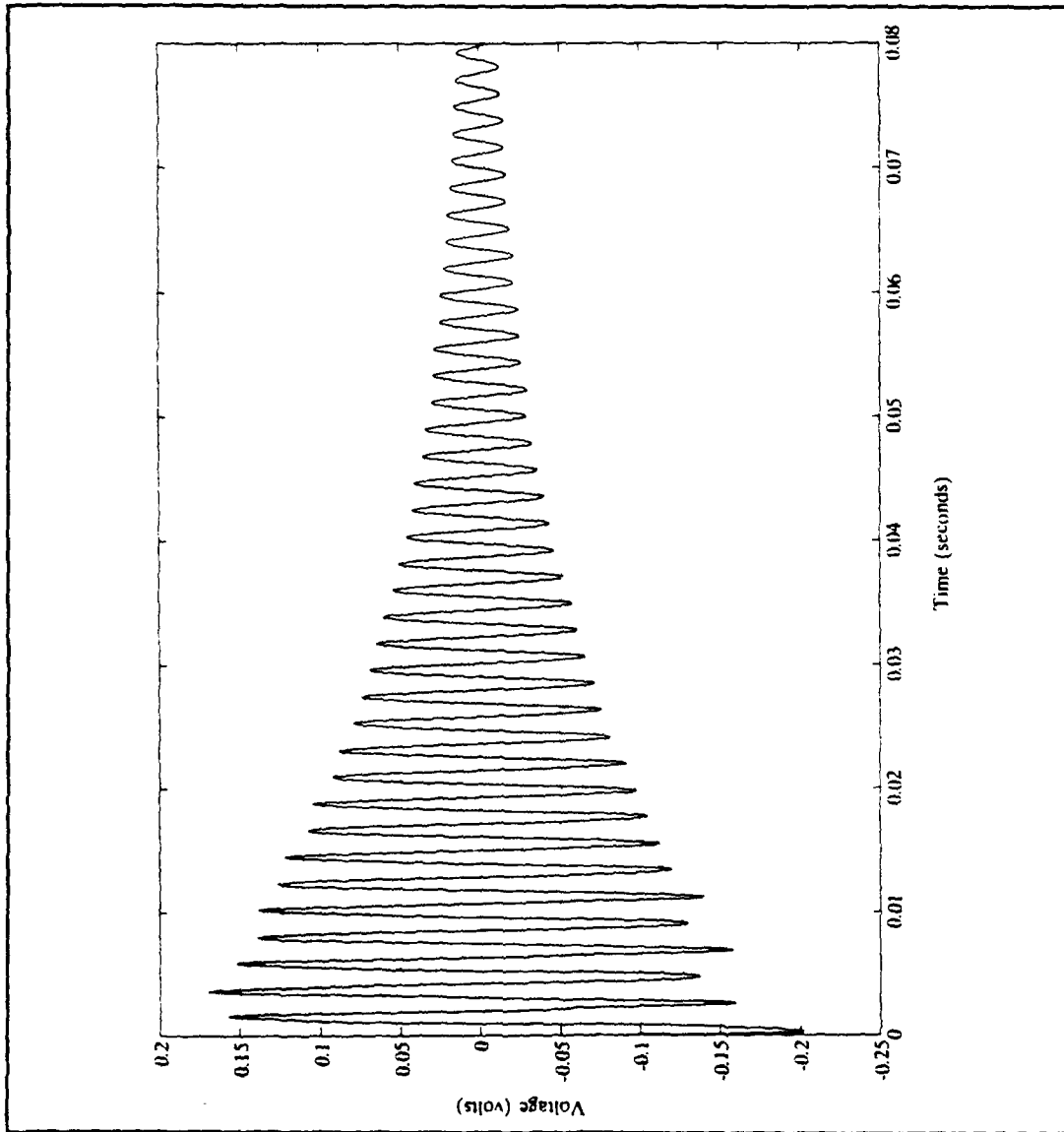


Fig.III.D.3 Time series plot of the 1-2-3 clapper constructed from acrylic. Note that the acrylic produces a usable signal for the entire record length.

E. CONSTRUCTION OF RESONATORS

A high degree of quality and precision was required in the construction of the resonators. In order for the experimental results not to deviate more than $\pm 1.0\%$ from the desired musical value, a tolerance of ± 0.002 inches on the interior diameters of the resonators was stipulated. To achieve this tolerance the following method was used to construct the resonators.

Initially, the two, three, and four-pitch resonators were started using the same process, utilizing a blank acrylic solid cylinder, seven inches long, cut from a three inch diameter acrylic rod. The blank was then placed on a three chuck lathe and a pilot hole, whose diameter was less than the smallest diameter (required for that particular resonator), was drilled through the cylinder. To obtain the desired tolerance, the requisite diameters were bored out using a boring bit attached to a boring bar. It should be noted that the diameter of the pilot hole would have to be large enough to accept the boring bar. Such that it was critical that the bored cavities be concentric, during the boring phase the cylindrical blank was not removed from the lathe and both diameters were bored from the larger diameter side. In the construction of all of our resonators, the step change from one diameter to the other occurred at the halfway point of the resonator. This completed the construction for the two-pitch resonators.

The three-pitch resonators were actually two separate but identical two-pitch resonators cut in half lengthwise. Each two-pitch resonator was cut longitudinally off centered and then milled down to the desired exterior diameter, such that the two halves were concentric. The interior diameters of the two and three-pitch resonators are given in Table III.A.2.

The four-pitch resonators were constructed in the same manner as the three-pitch resonators, except that instead of two identical halves each two-pitch resonator was of different interior diameters. The dimensions for the four-pitch resonator are given in Table III.C.1.

IV. EXPERIMENT

In this chapter, we discuss our experiment to test the theory. In the first two sections, we discuss the methods of detecting and exciting the sound. In the last two sections, we present the data and its analysis.

A. DETECTION

In this section, the methods used to obtain data will be discussed. This will include the equipment used and factors which could lead to experimental or random errors. Our desire was to capture a high quality free-decay signal for each of the frequencies of every resonator. Since each excitation of a resonator is an independent event, we required the ability to store multiple signals of a single resonator, for a detailed analysis at a later time. Additionally, without the use of an anechoic chamber, we wanted to ensure that the captured free-decay signal of each resonator was a true representation of that free-decay without the effects of outside influences. The detailed analysis included measurement of the period for each individual cycle, a computer generated FFT of for every decay signal, and a determination of the quality factor for each decaying signal.

There were several stipulated considerations involved in the obtaining of measurements for this thesis, that provided the criterion for our method. The basic requirement of determining the resonant frequencies for each of two, three, and four-pitch resonators to within ± 0.2 Hz was the primary driving factor. To capture these signals, we would require just the basics of acoustic signal measuring. Since the resonant frequency was our desired goal, we needed some type of an oscilloscope capable of displaying the decaying signal in such a manner that an accurate measurement of the periods could be made. Further equipment

required included a combination high pass/low pass filter to filter out undesired signals, and a microphone sensitive enough to respond to the excitation signal. However, the microphone must not be too sensitive, because we desire that the influence of background noise be kept to a minimum.

The first piece of equipment selected was the oscilloscope. The requirement to have the capability of storing numerous records made the Nicolet Digital Oscilloscope (NIC-310) the ideal choice for our work. The NIC-310 provided us the capability to record one separate signal after another on a 3.5" floppy disk and then at a later time retrieve the signal for analysis. The digital oscilloscope would sample 4000 data points for each single experimental run, regardless of the length of signal to be captured. Additionally, the NIC-310 has the capability to expand the x and y axis of a stored signal, on the screen, thus allowing a precise measurement of each of the 4000 data points, from the digital numerical display. After some initial experimentation using the NIC-310 while attempting to record data from a 1-5 slapper resonator (an original version without end effect corrections included), the average length of a good quality time series of the data signal was approximately 80 ms. Thus, for the measurement of all resonators the time per point setting used on the NIC-310 was 20 μ s. Of particular note is that, since the method used to measure the periods was to mark the zero crossings of the x axis for each cycle, the DC offset on the NIC-310 needed to be zero. It was discovered that the NIC-310 had a DC voltage drift of approximately 1 mV per minute. Therefore, the NIC-310 required a zeroing of the DC offset voltage after each experimental run. The selection of a acceptable microphone proved to be more complicated than the selection of the oscilloscope. The first microphone used was a Realistic #33-918 Dynamic Microphone. In the early stages of our work the Realistic appeared to be more than adequate for our measurements. However, later it was discovered that mass element of the Realistic produces a ring down effect. This

effect produces a frequency of approximately 200 to 300 Hz, with higher harmonics in the 600 and 1500 Hz range measured. This revelation suggested that use of the Realistic microphone could cause serious problems with the reliability of the recorded data. Since, the ring down frequency (fundamental and harmonics) falls in the middle of the theoretical frequency range of all the resonators of 300 to 700 Hz, we therefore disregarded the Realistic microphone. Our next selection was the General Radio microphone #1962-9610 with a #1560-P42 preamplifier and a #1560-P62 power supply. Test revealed that since the General Radio is of the electret type, the microphone did not produce the undesired ring down effect. However, the General Radio power supply did pick up and amplify 60 Hz noise. This 60 Hz noise occurs even though the power supply was on batteries, if the electrical power cord was not connected to the 120 V wall outlet. This was attributed to the lack of proper 60 Hz grounding on the building occupied by the lab. Therefore, in the course of this experiment the power supply was left plugged into the wall outlet while the power supply was running on batteries, to ground out the 60 Hz interference. Two additional types of microphones were tested to insure that the General Radio was indeed the best for our purposes. A Bruel-Kjaer type was tested but proved to be too sensitive to background noises to make it usable in our lab. Finally, a microphone was constructed using a Realistic Electret element, which cost all of one dollar. Upon comparison of test with the Bruel-Kjaer and the General Radio microphones, the Electret produced results that match up fairly well. However, since numerous measurement were to be carried out over an extended period, we decided that the General Radio microphone was better suited to our purposes. Since, the General Radio microphone provided us with a higher degree of reliability.

The final piece of equipment selected was the high pass/low pass filter. Two different filters were considered the Ithaco 1201 and the Krhon-Hite 3202R. Since, the General Radio preamplifier has the ability

to produce a gain of 10X (the desired gain to produce a reasonable amplitude to be measured on the NIC-310) the built in gain on the Ithaco would not be required. We tested both filters for internal noise and cutoff frequencies with the low pass filter set at 3000 Hz and the high pass set at 150 Hz. It was concluded that either filter would have been adequate for our purposes, but our decision to use the Krohn-Hite filter was based on the sharper cutoff frequencies. A diagram of the experimental setup is shown in Fig.IV.A.1.

The experimental method used to obtain the data was first to excite the resonator repetitively until a desirable signal was displayed on the oscilloscope, then save the signal on a 3.5" floppy disk. After a number of signals consider to be a fair representation of the decay signal were acquired, the best three individual signals were then recalled to the screen, the x and y axis were expanded and the measurement of period for each cycle was made to the nearest 0.01 ms (using the method of zero crossings as discussed previously). The time series plot of a typical decay signal (in this case the 1-3 slapper) is shown by Fig.IV.A.2. After the periods for each cycle were recorded, the average period over the entire length of the signal was calculated. From this average period the average resonant frequency was determined. The individual period values plotted in sequential order from time zero for one data run of the 1-3 slapper can be seen in Fig.IV.A.3. The record data stored on a disk was then used to produce a computer generated FFT of the time series using PCMATLAB as seen in Fig.IV.A.4 (for the same record as before). The frequency resolution of 12.5 Hz for the FFT was predetermined from the sampling frequency of the NIC-310. The sampling frequency used for our work was 50 kHz. This rather high frequency was necessary, due to the short time span of our signal, in order to obtain sufficient data points to reconstruct the signals and measure the periods within the desired accuracy. Our desire to have a computer generated FFT of the decay signal was to observed the frequency shifting of the overtones due to the

nonuniformity of the resonators. The arrows in Fig.IV.A.4 represent the overtones for the uniform resonator (i.e. a resonator with no step). Lastly, because it is not clear that the decay should be linear (Section V.B), we examined the logarithm of the voltage verses time. The decays were indeed found to be linear, and the quality factor Q for each resonator was determined using

$$Q = \frac{\omega}{2\alpha} , \quad (\text{IV.A.1})$$

where ω is the resonant frequency and α is the slope of the natural logarithm of the absolute value for the voltage amplitudes plotted verses time. Fig.IV.A.5 shows the plot used to determined α , for a sample resonator.

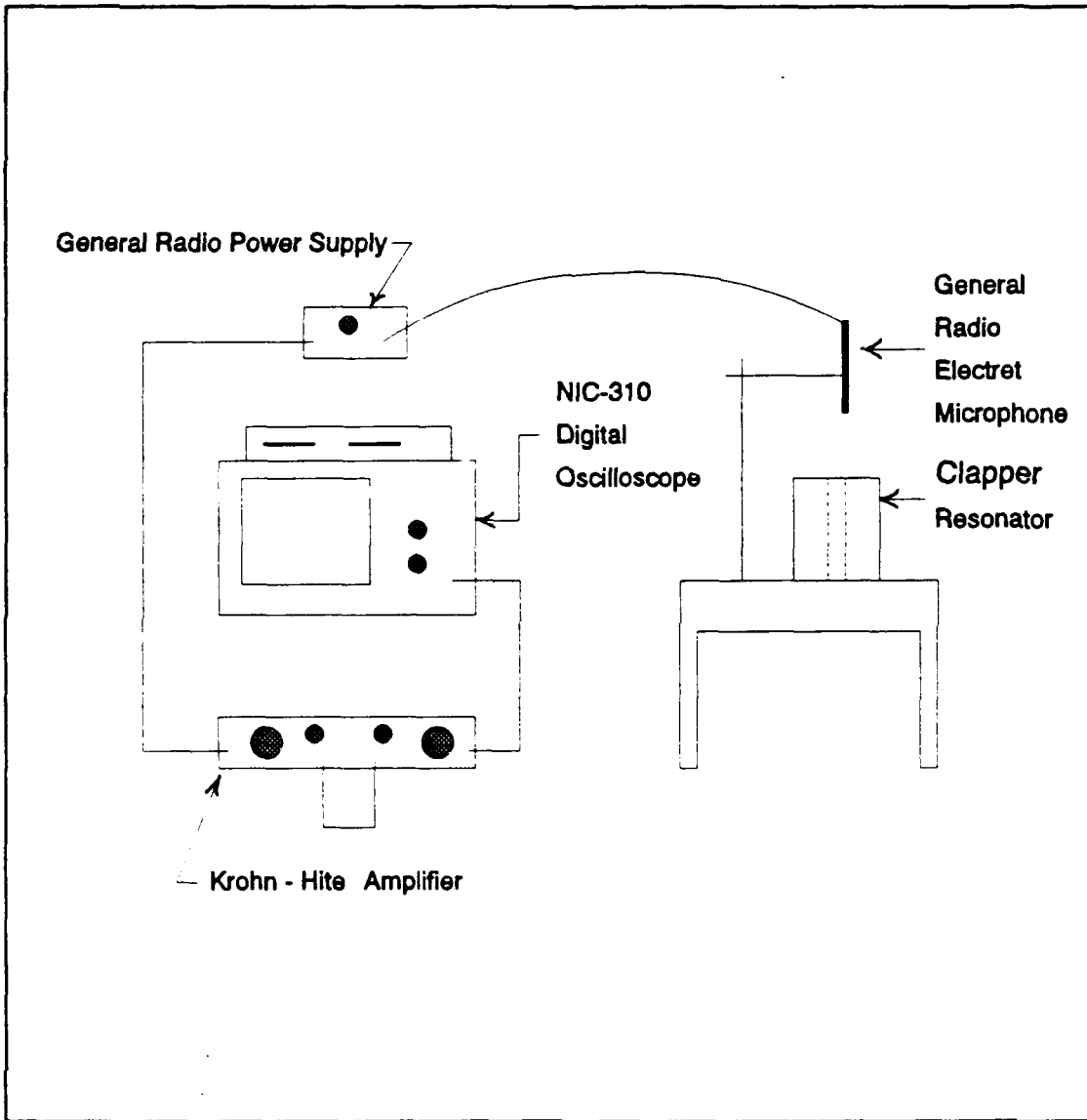


Fig.IV.A.1 Diagram of experimental setup

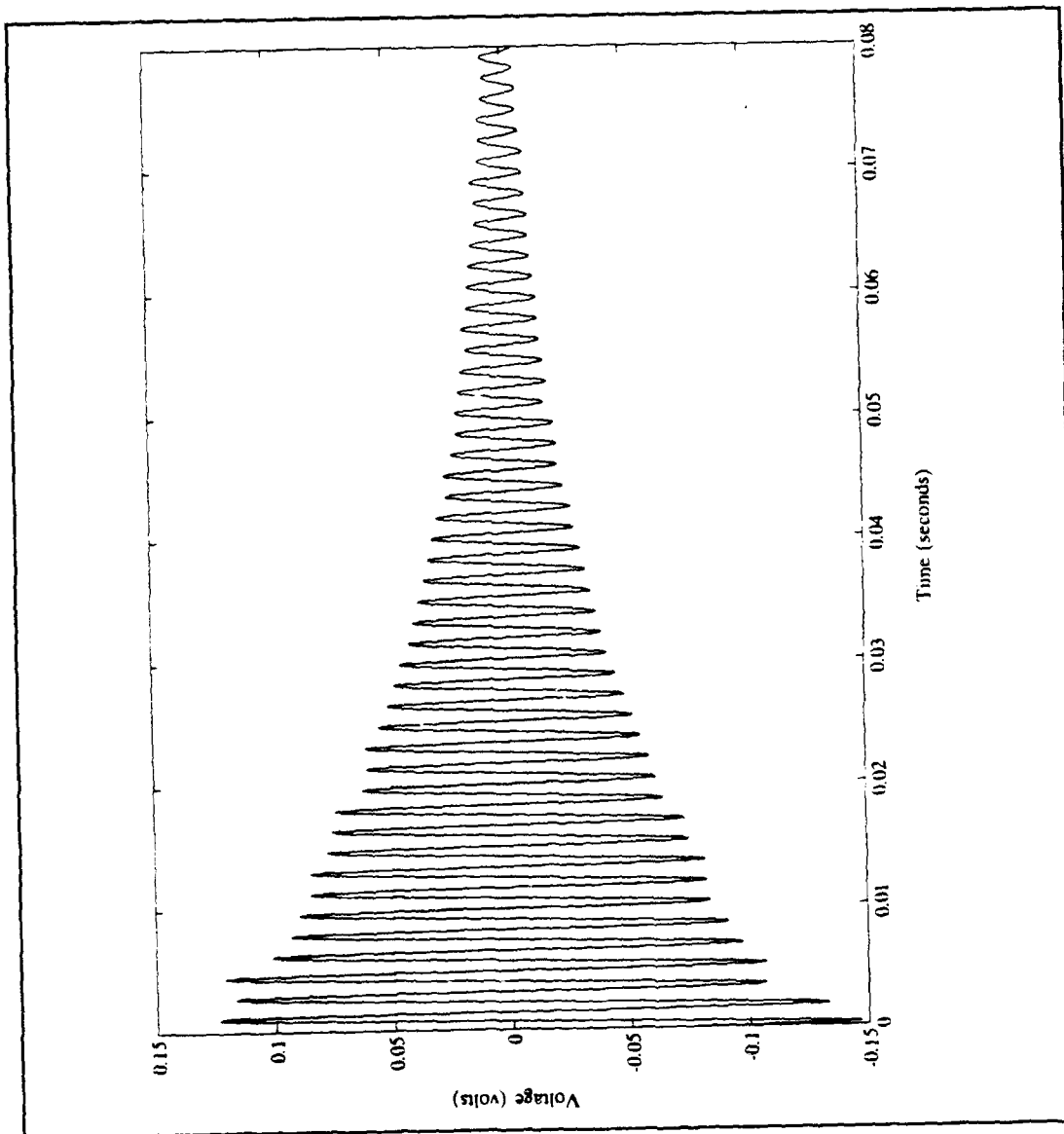


Fig.IV.A.2 Typical time series of the decay signal for a 2-pitch "slapper" resonator. This time series plot is the high frequency for a 1-3 resonator.

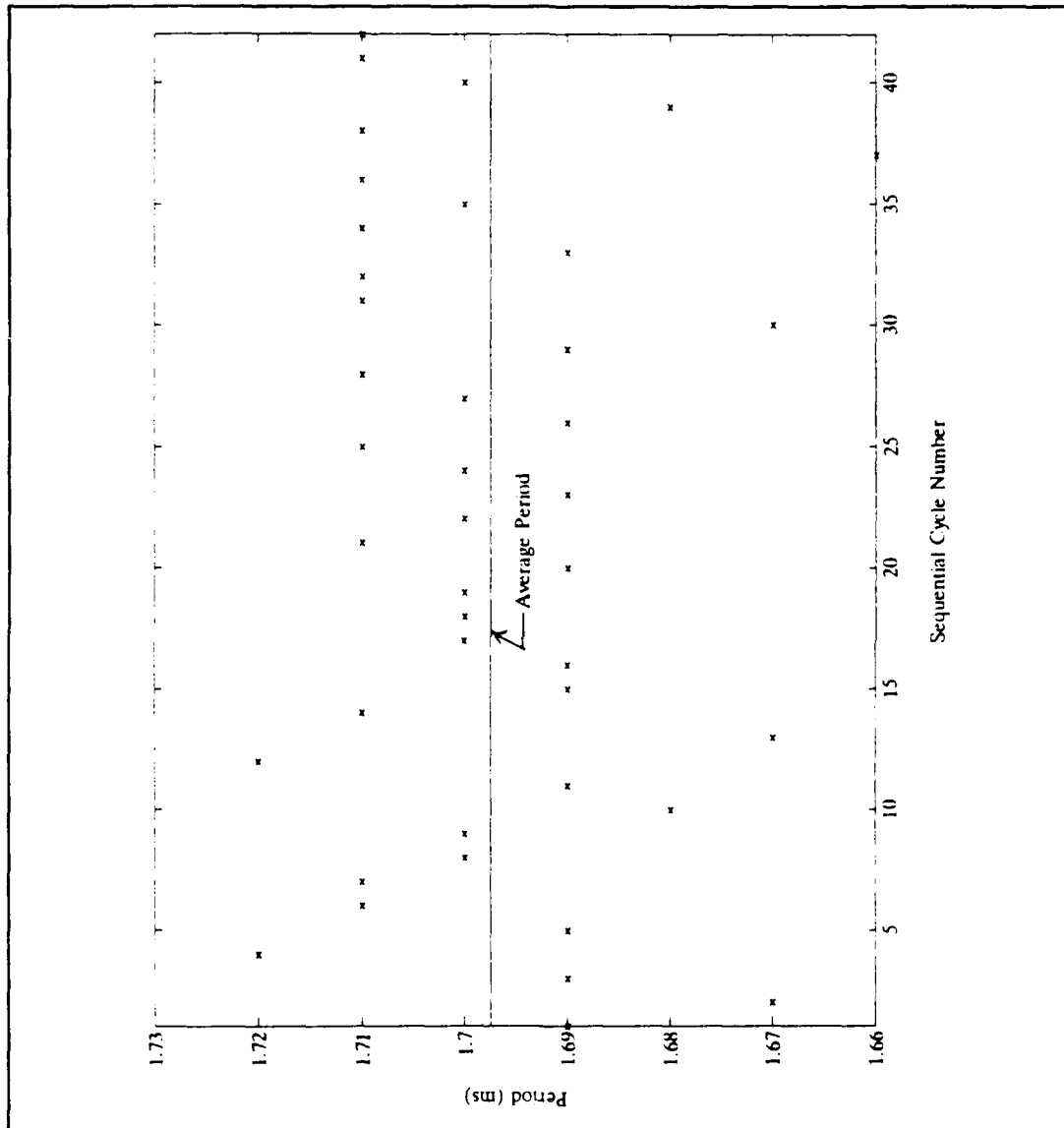


Fig.IV.A.3 Dispersion plot of the individual periods for each cycle of a typical 2-pitch "slapper" resonator. This plot is of the high frequency for a 1-3 resonator.

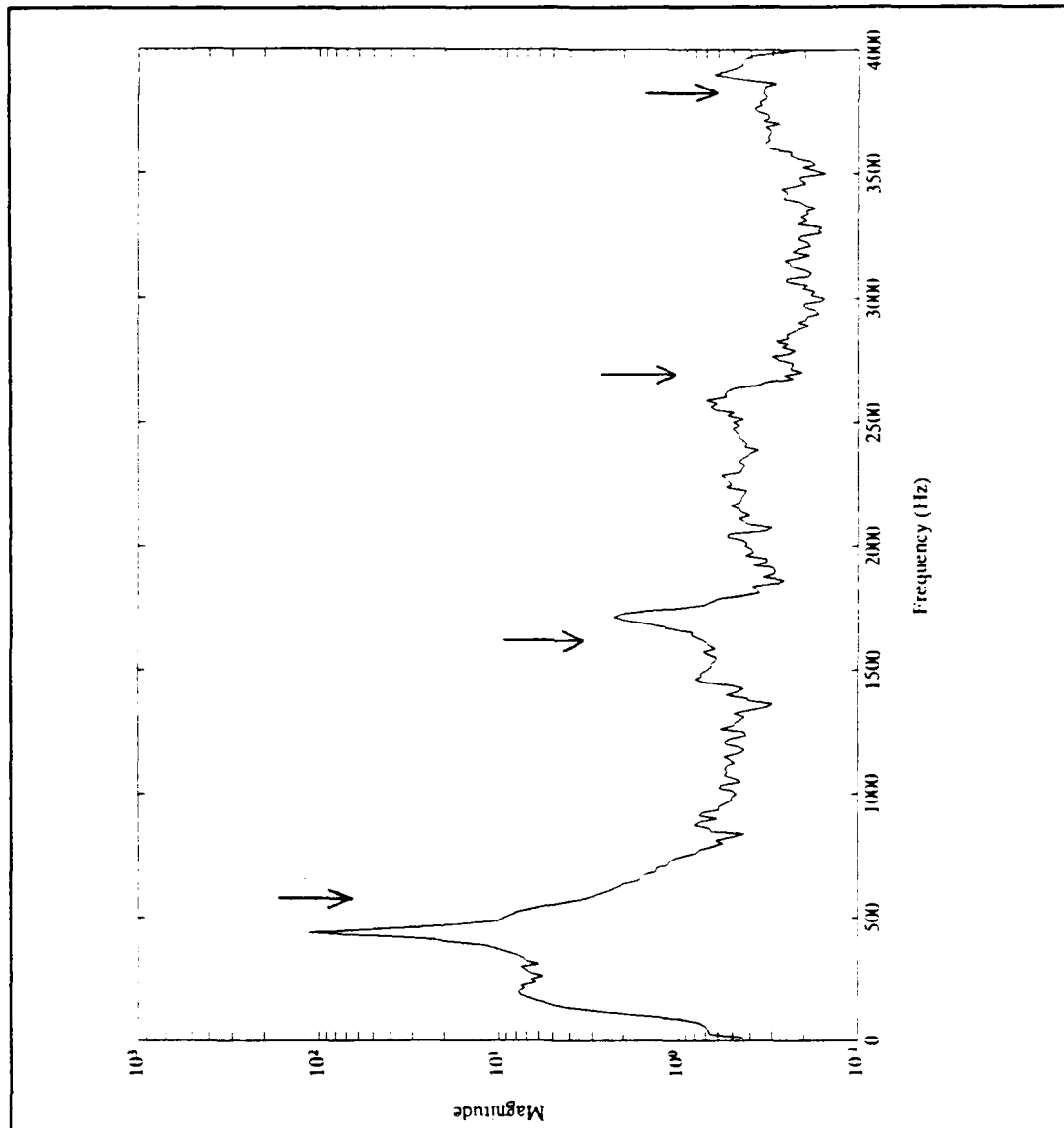


Fig.IV.A.4 Computer generated FFT plot using PCMATLAB for a typical 2-pitch "slapper" resonator. Note the frequency shifts of the overtones of the nonuniform case as compared to the overtones for the uniform case (arrows).

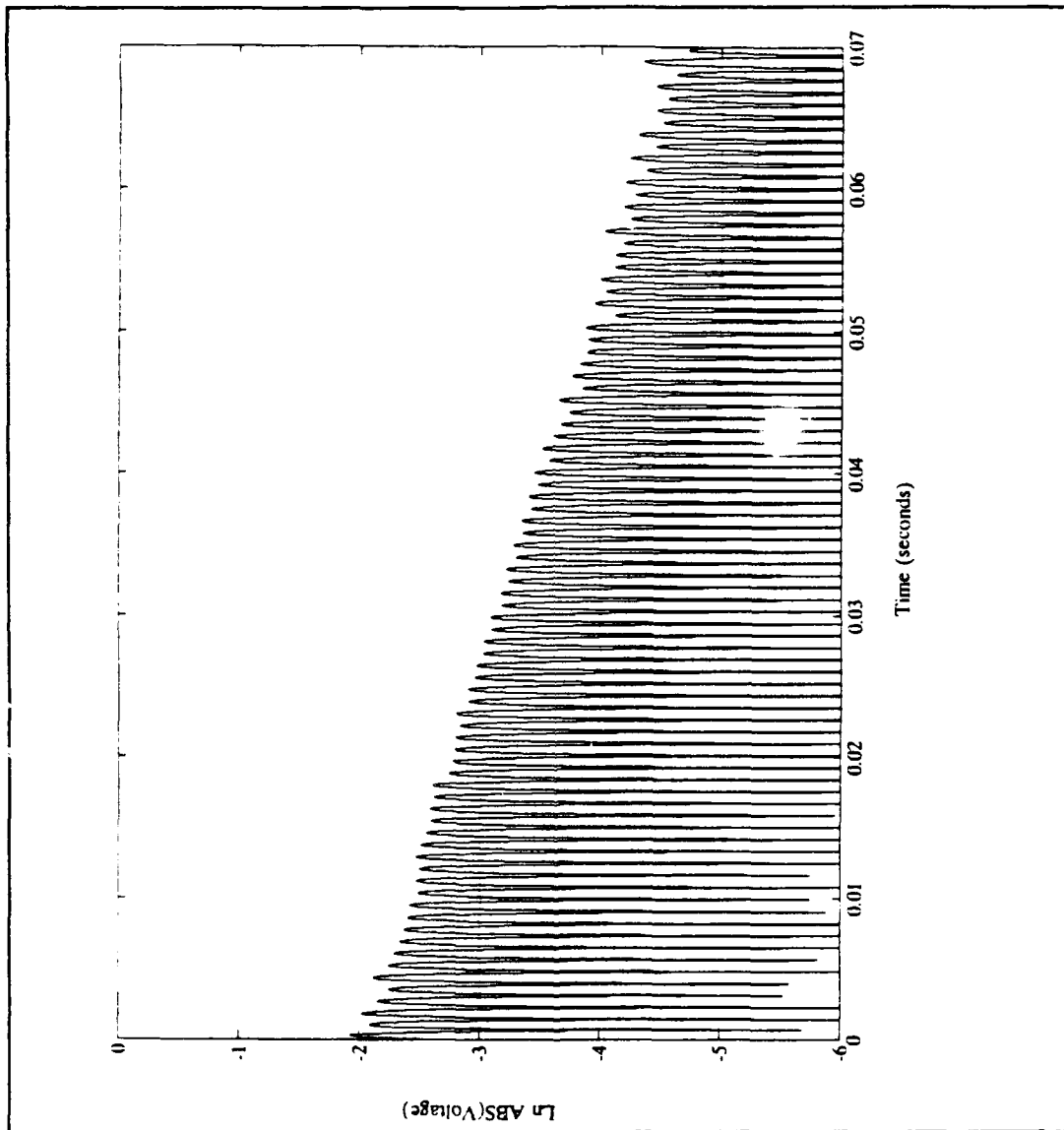


Fig.IV.A.5 Plot of the logarithm of the absolute voltage amplitude versus time. This plot was used to compute the Quality factor for a typical 2-pitch "slapper" resonator.

B. EXCITATION

It should be noted that for demonstration purposes, as discussed in Section I.B, that the palm of the hand can be used for excitation of the two-pitch resonator. However, in reality the hand excitation of the slapper, while producing usable data, proved to be a difficult method to reproduce continuously and required numerous experimental runs to acquire just one good signal. This was discovered to be a result of a changing in the boundary conditions at the end of the slapper caused by the palm of the hand not sealing the resonator completely. Additionally, after data comparison, it was observed that a small fraction of the palm of the hand entered into the interior of the resonator, thereby changing the acoustic length of the slapper. This changing of the acoustic length of the slapper was unacceptable for our measurements, since this produced a change in the resonant frequency that would not be reproducible from data run to data run. Therefore, a different method of exciting the slapper was required that produced the same boundary conditions every time. It was observed that if a #12 rubber stopper was used to excite the slapper by striking the stopper against the end of the slapper, the output signal was not only easier to reproduce time and time again but that the signal was exceptionally clean. This clean signal meant that the entire length of the signal from time zero to 80 ms was now usable. By comparison of Fig.IV.B.1, a time series of the 1-8 slapper using excitation by the palm of the hand and Fig.IV.B.2 where excitation was by use of a #12 stopper, it can be seen that the signal in Fig.IV.B.2 is more desirable for experimental purposes.

For the case of excitation of the three and four-pitch resonators the method described in Section I.B was effective in producing good quality data.

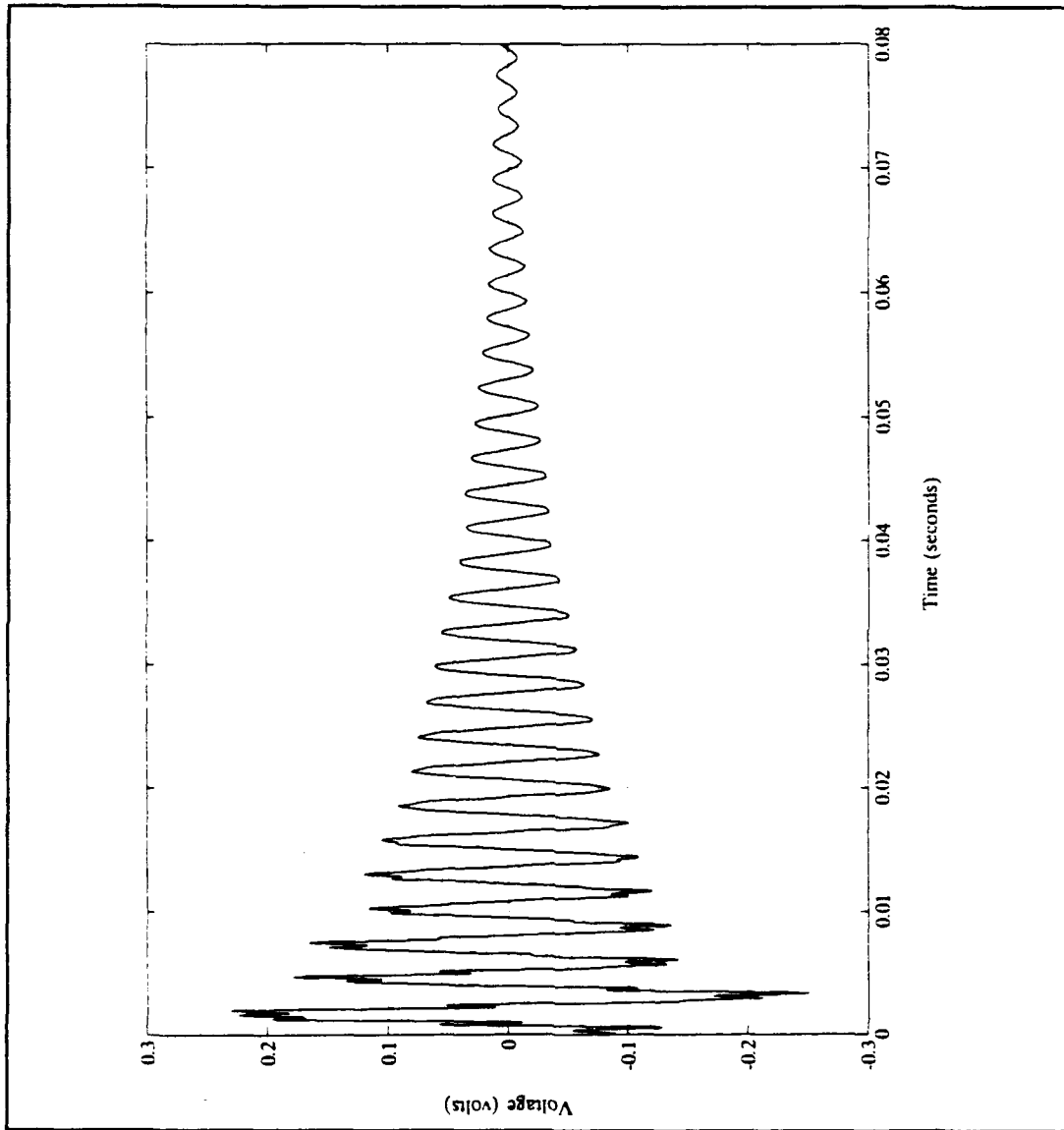


Fig.IV.B.1 Times series decay plot of the low frequency for a 1-8 slapper resonator excited by using the palm of the hand.

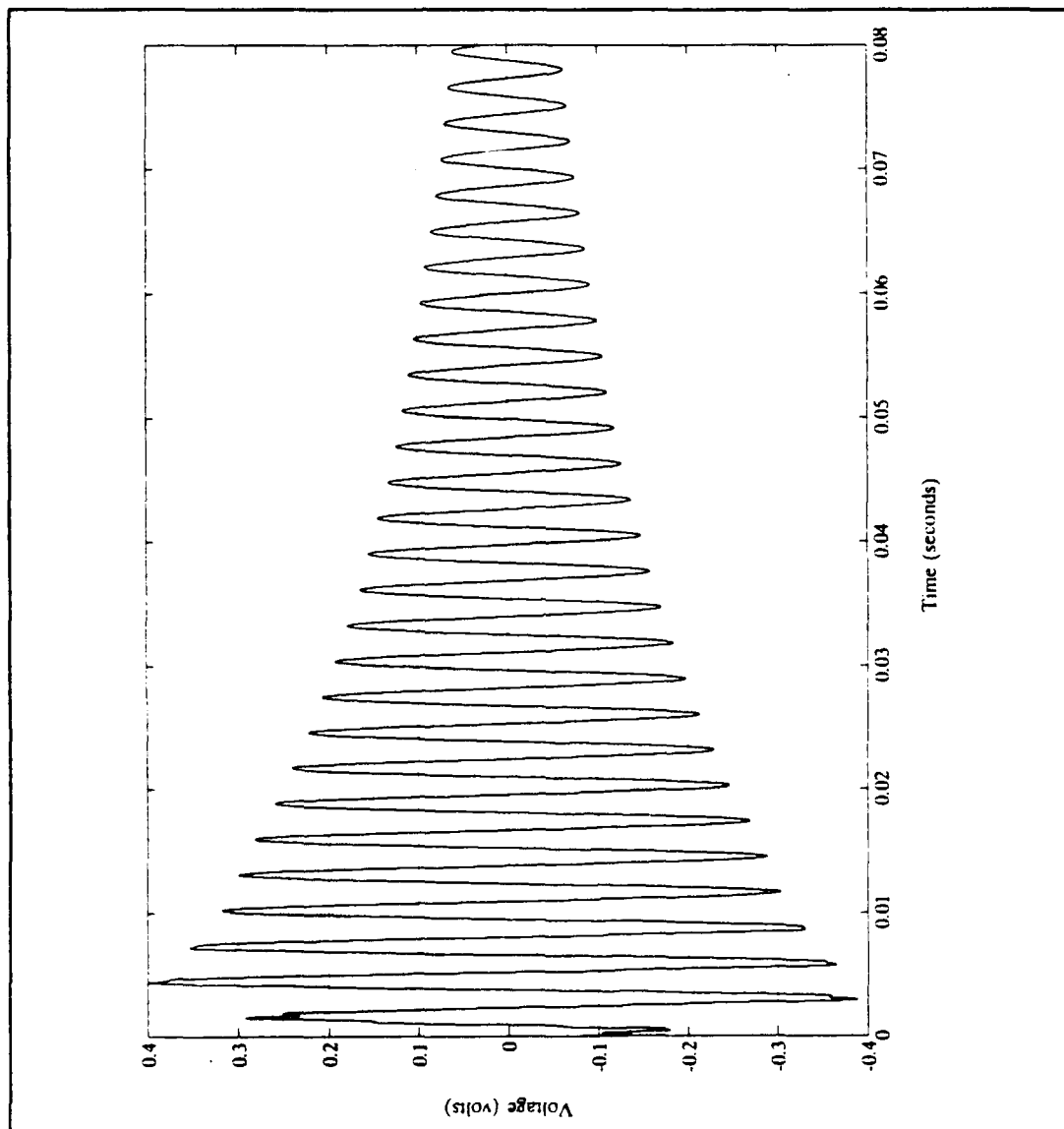


Fig.IV.B.2 Times series plot of the low frequency for a 1-8 slapper resonator excited using a #12 rubber stopper.

C. DATA

In this section the data acquired and reduced as discussed in Section IV.A will be presented. For each resonator, three separate experimental runs were used for the data reduction of each particular frequency. After the initial decay signal was recorded the methods discussed in Section IV.A were used to obtain the results included in Table IV.C.1 through Table IV.C.8. To clarify the presented data, the average periods were measured using an average of 40 consecutive cycles in the case of the higher frequencies of the resonators and an average of 28 consecutive cycles for the lower frequencies. From the average period the average resonant frequency was then calculated. The quality factor was then determined in the manner discussed in Section IV.A.

As can be observed from Table IV.C.1 through Table IV.C.8, there is relatively good agreement between the average resonant frequencies for each experimental run for a given resonator. Nominally, the difference in resonant frequencies appears to less than 0.4 Hz, this is as expected due to the experimental errors encountered, which would affect each independent run to some degree. The factor that proved to be the most sensitive and caused large deviations in the resonant frequencies between each experimental run was the air temperature. The temperature had little effect when the accuracy was required to be within one hertz. However, when accuracy was required to be within tenths of hertz the temperature was the limiting factor. To overcome this problem required the cycling through the frequencies of each resonator by capturing one record for a particular frequency then capturing one record for the next frequency. This method was repeated until three records had been captured for each frequency.

This method proved to be successful and allowed the average resonant frequencies to be computed from experimental runs whose deviations were in the tenths of hertz. The quality factors for the all of the resonators were approximately in the 40 to 60 range.

Table IV.C.1 Data from the 1-3 Slapper Resonator.

Record	Period Average (ms)	Resonant Frequency Average (Hz)	Quality Factor
S1345	2.136	468.3	51
S1346	2.136	468.2	59
S1348	2.135	468.5	52
S3141	1.698	588.9	52
S3142	1.698	589.0	54
S3144	1.697	589.2	50

Table IV.C.2 Data from the 1-5 Slapper Resonator

Record	Period Average (ms)	Resonant Frequency Average (Hz)	Quality Factor
S1525	2.385	419.2	44
S1529	2.386	419.2	47
S1530	2.386	419.1	43
S5131	1.594	627.3	66
S5133	1.593	627.7	69
S5135	1.594	627.6	64

Table IV.C.3 Data from the 1-8 Slapper Resonator

Record	Period Average (ms)	Resonant Frequency Average (Hz)	Quality Factor
S1822	2.895	345.4	35
S1823	2.895	345.4	42
S1803	2.894	345.5	40
S8104	1.453	688.3	47
S8105	1.454	688.5	48
S8106	1.453	688.4	47

Table IV.C.4 Data from the 1-2-3 Clapper Resonator. The records correspond to the lower, middle and high frequency, respectively.

Record	Period Average (ms)	Resonant Frequency Average (Hz)	Quality Factor
C12353	2.158	463.4	41
C12355	2.155	464.0	42
C12356	2.157	463.6	43
C23157	1.910	523.6	45
C23159	1.910	523.5	43
C23160	1.912	523.2	44
C32146	1.719	581.7	40
C32147	1.718	581.9	40
C32162	1.718	581.8	39

Table IV.C.5 Data from the 1-3-5 Clapper Resonator. The records correspond to the lower, middle and high frequency, respectively.

Record	Period Average (ms)	Resonant Frequency Average (Hz)	Quality Factor
C13526	2.391	418.3	50
C13527	2.391	418.3	50
C13529	2.392	418.1	48
C35131	1.925	519.4	41
C35132	1.925	519.6	42
C35133	1.926	519.2	42
C53136	1.601	624.6	39
C53149	1.602	624.4	36
C53150	1.602	624.4	36

Table IV.C.6 Data from the 1-5-8 Clapper Resonator. The records correspond to the lower, middle and high frequency, respectively.

Record	Period Average (ms)	Resonant Frequency Average (Hz)	Quality Factor
C15872	2.892	345.8	44
C15875	2.890	346.0	41
C15878	2.891	345.9	45
C58173	1.963	509.4	53
C58176	1.965	508.9	52
C58179	1.963	509.4	50
C85174	1.454	687.8	39
C85177	1.453	688.2	34
C85180	1.454	687.8	40

Table IV.C.7 Data from the 1-2-3~~4~~-4 Clapper Resonator. The records correspond from the lowest to the highest frequency, respectively.

Record	Period Average (ms)	Resonant Frequency Average (Hz)	Quality Factor
C4120	3.311	302.0	36
C4124	3.310	302.1	36
C4128	3.308	302.3	41
C4221	2.929	341.4	42
C4225	2.932	341.1	45
C4229	2.931	341.2	42
C4322	2.759	362.4	38
C4326	2.761	362.2	36
C4330	2.761	362.2	38
C4423	2.484	402.6	38
C4427	2.486	402.3	38
C4431	2.485	402.4	39

Table IV.C.8 Data from the 5-6b-7-8 Clapper Resonator. The records correspond from the lowest to the highest frequency, respectively.

Record	Period Average (ms)	Resonant Frequency Average (Hz)	Quality Factor
C4505	2.226	449.2	49
C4509	2.225	449.4	43
C4513	2.226	449.2	56
C4602	2.090	478.5	42
C4610	2.089	478.7	43
C4614	2.090	478.5	41
C4715	1.754	570.1	52
C4716	1.755	569.8	54
C4717	1.755	569.8	57
C4804	1.671	598.4	47
C4808	1.671	598.4	44
C4818	1.671	598.4	48

D. ANALYSIS

In this final section of the experimental chapter the final results from the research conducted are displayed in Table IV.D.1 through Table IV.D.3. The average frequencies are calculated by taking the average of the three resonant frequencies (Table IV.C.1 through Table IV.C.8) measured for each particular frequency of each resonator. The relative frequency is simply the ratio of the high frequency to the low frequency which is the musical interval or step of the resonator.

It can clearly be seen that, of the resonators constructed for testing by using the design criteria given by Section III.A through Section III.C for the two, three, and four-pitch resonators, respectively, the relative frequencies were in good agreement with the desired musical intervals. It should also be noted that by incorporating end effects into our design of the resonators, we were able to get the experimental data to agree with the desired musical value to within our predetermined criterion of less than roughly one percent deviation.

Table IV.D.1 Final Results for the 2-Pitch Resonators

Resonator	Low Frequency (Hz)	High Frequency (Hz)	Relative Frequency	Deviation from Musical Value
1-3	468.3	589.0	1.258	- 0.2 %
1-5	419.2	627.5	1.497	- 0.1 %
1-8	345.4	688.4	1.993	- 0.4 %

Table IV.D.2 Final results for the 3-Pitch Resonators

Resonator	Low Frequency (Hz)	Higher Frequency (Hz)	Relative Frequency	Deviation from Musical Value
1-2-3	463.7	523.4	1.129	+ 0.6 %
		581.8	1.255	- 0.4 %
1-3-5	418.2	519.4	1.242	- 1.4 %
		624.5	1.493	- 0.4 %
1-5-8	345.9	509.2	1.473	- 1.7 %
		687.9	1.989	- 0.6 %

Table IV.D.3 Final results for the 4-Pitch Resonators.

Resonator	Frequency (Hz)	Relative Frequency	Deviation from Musical Value
1-2-3♭-4	302.1	1	----
	341.2	1.129	0.6 %
	362.3	1.199	0.8 %
	402.4	1.332	- 0.2 %
5-6♭-7-8	449.2	1.487	- 0.8 %
	478.5	1.584	- 0.2 %
	569.8	1.886	- 0.1 %
	598.4	1.987	- 0.9 %

V. CONCLUSIONS AND FUTURE WORK

In this chapter, we summarize the results and then discuss possible future research involving nonuniform resonators.

A. CONCLUSIONS

We have investigated piecewise uniform acoustic resonators whose configurations can be simply and quickly altered, leading to changes in the frequency. Various resonators have been constructed such that the frequencies correspond to musical notes. There are two types of resonators: single-piece "slappers", whose ends are slapped in order to generate the sound, and double-piece "clappers", which are clapped together while one set of ends rests on a smooth surface. The apparatus are primarily useful as educational demonstrations of the effects of nonuniformity on standing wave modes. The demonstrations have the advantage of being inexpensive and simple to perform.

On an elementary level, the demonstrations can be appreciated as an effect of symmetry-breaking. The explanation is not elementary, however. We have presented three theoretical approaches: matching solutions of the wave equation, applying the energy method of Rayleigh, and applying the theorem of adiabatic invariance. The second and third approaches, which are perturbative and yield the same result, offer physical explanations. The first approach, which is more accurate, was employed in the design of the resonators. We obtained excellent agreement with this theory when end effects were approximately included, and observed small but significant deviations from the perturbative theory.

B. FUTURE WORK

There are several possible avenues for future research regarding piecewise uniform resonators. In this section, we briefly discuss some of these.

The standard theory is not exact, although our data show no indication of a breakdown of the theory. It would be interesting to perform a careful experiment to attempt to observe deviations. It may be that the breakdown only occurs when the length of the resonator becomes comparable to the diameter; that is, when the system is no longer approximately one-dimensional. Analytically, one could begin with the exact two-dimensional transmission step theory of Morse and Ingard (1968). This may be relevant.

We are not aware of any quantitative experiment in the breakdown of adiabatic invariance. A piecewise uniform resonator with a movable step or length may be a feasible candidate. As discussed in Section II.F, when the discontinuity in area is large, pairs of modal frequencies can be separated by a small amount (Fig.II.F.1). Exciting one mode and then altering the geometry such that the frequencies of this and another mode become close, may lead to a partial excitation of the nearby mode. This would be a breakdown of adiabatic invariance. It may inherently be connected to a breakdown of the constancy of E/ω for the original mode.

Finally, we consider a question regarding the free decay of a mode of a closed-closed piecewise uniform resonator. Due to the different areas, the quality factors of the individual uniform sections will differ. One may then wonder whether or not a mode decays as a pure exponential. Specifically, consider a large widening step halfway along the resonator ($A_2 \gg A_1$ and $\alpha = 1/2$ in Fig.II.A.1). By the results of Section II.F, the fundamental and first overtone have nearby frequencies. Furthermore, the results suggest that the behavior can be represented as a system of two coupled identical oscillators with different damping parameters. It is

not difficult to show that, according to this model, the decay of either normal mode is not purely exponential. However, the effect is significant only if the coupling is weak (or if the frequencies of the modes deviate by a small amount). It would be interesting to analytically and experimentally investigate the free decay of a sound mode in the geometry described above. Our experience is that the typical intuition of an acoustician is that the decay is always purely exponential, regardless of the geometry.

REFERENCES

Crawford, Frank S., "Singing Corrugated Pipes," *American Journal of Physics*, v.42, pp.278-288, 1974.

Crawford, Frank S., "Elementary Examples of Adiabatic Invariance," *American Journal of Physics*, v.58, pp.337-344, 1990.

Garrett, Steven L., "Resonant Acoustic Determination of Elastic Moduli," *Journal of the Acoustic Society of America*, v.88, pp.210-221, 1990.

Landau, L.D. and Lifshitz, E.M., *Fluid Mechanics*, pp.252-253, Pergamon Press, New York, 1959.

Morse, Philip M., *Vibration and Sound*, pp.246-248, Acoustical Society of America, Woodbury, New York, 1976.

Morse, Philip M., and Ingard, K.Uno, *Theoretical Acoustics*, pp.488-490, McGraw-Hill, New York, 1968.

Pierce, Allan D., *Acoustics*, p.348, Acoustical Society of America, Woodbury, New York, 1989.

Rayleigh, J.W.S, *Theory of Sound*, Vol. II (1896), pp.66-68, Dover, New York, 1945.

Szeszol, Steve, "Pipe Music," *Physics Teacher*, v.25, pp.173-175, 1987.

INITIAL DISTRIBUTION LIST

	<u>No. Copies</u>
1. Defense Technical Information Center Cameron Station Alexandria, VA 22304-6145	2
2. Dr. Bruce C. Denardo, Code PH/De Department of Physics Naval Postgraduate School Monterey, CA 93943-5002	5
3. LT Steven L. Alkov Department Head Class 120 Surface Warfare Officers School Command Newport, RI 02841-5012	1
4. Library, Code 52 Naval Postgraduate School Monterey, CA 93943-5002	2
5. Prof. Anthony A. Atchley, Code PH/Ay Chairman Engineering Acoustics Academic Committee Naval Postgraduate School Monterey, CA 93943-5002	1
6. Prof. Steven L. Garret, Code PH/Gx Department of Physics Naval Postgraduate School Monterey, CA 93943-5002	1
7. Dr. Seth Putterman UCLA Physics Dept. Los Angeles, CA 90024-1547	1
8. Prof. Steven P. Baker, Code PH/Ba Department of Physics Naval Postgraduate School Monterey, CA 93943-5002	1
9. Prof. Andres Larraza, Code PH/La Department of Physics Naval Postgraduate School Monterey, CA 93943-5002	1